7-2008

ESTIMATION OF VEHICLE MASS AND ROAD GRADE

Tejas Ghotikar
Clemson University, tejasghotikar@gmail.com

ESTIMATION OF VEHICLE MASS AND ROAD GRADE

A Thesis
Presented to
the Graduate School of
Clemson University

In Partial Fulfillment
of the Requirements for the Degree
Master of Science
Mechanical Engineering

---

by
Tejas Ghotikar
August 2008

Accepted by:
Dr. Ardalan Vahidi, Committee Chair
Dr. Lonny Thompson
Dr. Beshah Ayalew

Abstract

This thesis describes development of a real-time-implementable algorithm for simultaneous estimation of a heavy vehicle's mass and time-varying road grade and its verification with experimental data. Accurate estimate of a heavy vehicle's mass is critical in several vehicle control functions such as in transmission and stability control. The goal is to utilize the standard signals on a vehicle in a model-based estimation strategy, as opposed to a more costly sensor-based approach. The challenge is that unknown road grade complicates model-based estimation of vehicle mass and therefore the time-varying grade should be estimated simultaneously. In addition an estimate of road grade may be used as a feedforward input to transmission control and cruise control systems enhancing their responsiveness.

The vehicle longitudinal dynamics model (F=ma) forms the core of this model-based approach. Mathematically this is a single equation with one unknown parameter (mass) and one time-varying input disturbance (grade). The goal is to estimate the constant parameter and time-varying grade by using engine torque and speed, vehicle speed and transmission state. The problem is fundamentally difficult because of i) variation of grade over time ii) lack of "rich" data during most of vehicle's cruise time, iii) uncertainty about available traction force during gear-shift periods and braking, and iv) low signal-to-noise ratio for vehicle acceleration signal.

We have tested two independent estimation schemes using experimental data sets provided by Eaton Corporation. The first algorithm uses recursive least square with two forgetting factors for simultaneous estimation of mass and grade. The second algorithm is a two-stage scheme which cascades a Lyapunov-based nonlinear estimator next to a recursive least square scheme. These algorithms were conceived in our group in the past; however they needed modification and refinements for robust real-time implementation. After these

refinements, the modified algorithms are capable of generating estimates for mass and time-varying road grade which are more accurate in realistic scenarios and for most part of the vehicle run. More specifically we are able to generate very accurate estimates of road grade, when the clutch is fully engaged and we have proposed fixes that improve the quality of estimates even during periods of gear change. Provided persistence of excitations we are able to generate accurate estimates of mass which in turn improves the quality of grade estimate. It is important to robustify initialization of algorithm 1 further which is now sensitive to an initial batch size; a task listed in the future work. Algorithm 2 does not rely on an initial batch and therefore is expected to be adopted as the preferred approach for implementation.

After an overview in Chapter 1, development and verification of the vehicle longitudinal dynamics model and the first proposed methodology a recursive least square scheme with multiple forgetting for estimation of mass and time-varying grade are described in Chapter 2. The algorithm required a number of modification from its originally developed form; Chapter 3 explains the changes made to the original algorithm and the results obtained for different sets of experimental data provided by Eaton. Chapter 4 outlines a second two-stage estimation algorithm; and chapter 5 summarizes the modifications and refinements made to second algorithm and the improved results obtained using this algorithm. A description of the remaining issues and directions for improvement concludes the thesis.

Acknowledgment

The completion of my master's thesis would not have been possible without the help and support of several individuals. In first place I would like to express my sincere appreciation and gratitude to my advisor Dr. Vahidi for his continuous support, excellent advising and guidance for my research. Apart from good advisor, his effective way of teaching makes him one of my favorite teachers. I would like to thank other committee members Dr. Thompson and Dr. Ayalew for reviewing and providing invaluable feedback on my research work.

I would like to thank Advance Control & Automation group of Eaton Corporation for funding the project I was involved. I would like to thank Dr. Song from Eaton Corporation for working closely on this project and providing invaluable suggestions and help. I would also like to appreciate the help from Dr. McIntyre from Western Kentucky University for his help regarding my research work.

I am very grateful to the Department of Mechanical Engineering for providing very good facility for my research and financial help for first year of my study here at Clemson. I would like to express my gratitude to the faculties of the Mechanical Engineering Department for the help and knowledge I received during the courses I attend at Clemson University.

I would like to express my gratitude to all my friends for their support. In particular I would like to thank Indrasen, Saurabh and Judhajit for their help. I would also like to thank my roommates Ankur and Parikshit for making my stay at Clemson full of unforgettable memories.

Lastly but most importantly, I would like to thank my parents Jayant Ghotikar and Nilam Ghotikar for their continuous encouragement, support and love. I would like to dedicate this thesis to them.

Table of Contents

List of Tables

List of Figures

Chapter 1

Introduction

1.1 Introduction

In vehicle control, many control decisions can be improved if the unknown parameters of the vehicle such as mass of the vehicle, coefficient of rolling resistance, drag coefficient and external disturbances such as road grade can be estimated. Accurate estimation of the mass of a heavy duty vehicle (HDV) is particulary important as it can vary as much as 400% depending on the load it carries [8], [9]). Road grade is a major source of external loading [4] for heavy vehicle and is normally unknown. An anti-lock brake controller relies on an estimate of mass and road grade for calculating vehicle's cruise speed which is necessary for estimation of wheel slip. The engine control unit (ECU) can also utilize an accurate estimate of the road grade for estimating the engine torque which may reduce the need for in-line torque-meters [31]. In longitudinal control of automated vehicles, knowledge of the participating vehicle mass and road grade is necessary for avoiding issuing infeasible acceleration and braking commands [3]. Moreover, mass estimation is essential to the engine control unit (ECU) for reduced emission, and to transmission control for reduced gear hunting. The closed loop experiments performed by Yanakiev et al.

[33] indicate that the longitudinal controllers with fixed gains have limited capability in handling large parameter variations of an HDV. Therefore it is necessary to use an adaptive control approach with an implicit or explicit online estimation scheme for estimation of unknown vehicle parameters. Application of adaptive controllers that compensate for vehicle parameter variations has been presented in a number of references including in [12], [15], [29], and [17].

This thesis describes development of a real-time-implementable algorithm for simultaneous estimation of a heavy vehicle's mass and time-varying road grade and its verification with experimental data. The goal is to utilize the standard signals on a vehicle in a model-based estimation strategy, as opposed to a more costly sensor-based approach. The challenge is that unknown road grade complicates model-based estimation of vehicle mass and therefore the time-varying grade should be estimated simultaneously. In addition an estimate of road grade may be used as a feedforward input to transmission control and cruise control systems enhancing their responsiveness. The problem is fundamentally difficult because of i) time-varying grade disturbance ii) lack of persistent excitations during most of vehicle's cruise time, iii) uncertainty about available traction force during gear-shift periods and braking, and iv) low signal-to-noise ratio for vehicle acceleration signal.

1.2 Existing Methods for Estimation of Vehicle Mass and Road Grade

Importance of vehicle mass and road grade estimation has led to considerable research in this area in the past few years. Different sensor-based and model-based approaches have been proposed: In sensor-based methods the time-varying grade is typically estimated using sensor data such as an accelerometer [18] or GPS receiver [4], then a con-

ventional parameter estimation algorithm is utilized for estimation of the mass [32]. The drawback of sensor-based estimation is the cost and added complexity of extra sensors and therefore is not the preferred industry approach. A model-based estimation strategy on the other hand, uses existing signals from vehicle Control Area Network (CAN) and is a much cheaper alternative to sensor based estimation. Standard signals such as engine torque, vehicle speed, gear number, and gear shifting progress are utilized in a model based-estimator along with a model of longitudinal or lateral dynamics of the vehicle.

In particular model-based methods for simultaneous estimation of vehicle mass and road grade have been proposed recently. In a series of papers [26, 28, 30], Vahidi et al. have provided a method for simultaneous estimation of mass and time-varying grade using a novel recursive least square (RLS) method. In particular since standard RLS with a single forgetting factor was not capable of estimation of a constant mass and time-varying grades, an RLS with multiple forgetting factors was formulated. It was demonstrated, with both simulated and some test data, that incorporating two distinct forgetting factors could be effective in resolving the difficulties in estimating mass and time-varying grade. In a different approach presented in [26], a Lyapunov-based input observer is used to generate an estimate of the road grade given an initial estimate of the vehicle mass.

To address some of the standing issues of RLS with forgetting, McIntyre et al. [16] have proposed a two-stage Lyapunov based estimation approach, which combines a RLS strategy for mass estimation and nonlinear Lyapunov-based strategy for grade estimation. In its first stage, a least-squares estimator, based on the vehicle longitudinal dynamic model was developed which determined an estimate of the vehicle mass and a constant estimate of the road grade. Due to the time-varying nature of the road grade (which negatively influences the road grade estimate), a nonlinear estimator (see [20] and [2]) was then developed to provide a more accurate estimate of the road grade. Specifically, the HDV's mass was first determined by the adaptive least-squares estimator, then the mass estimate was utilized

by the nonlinear estimator to provide an estimate of time-varying road grade. Experimental results were presented illustrating the validity of the estimation strategy when the *persistence of excitation* was guaranteed. A filter augmented with the least-square estimator for the mass reduced the numerical difficulties that arose due to the noisy acceleration signal and was an improvement over the integration technique proposed in [30]. Moreover the nonlinear observer utilized for the road grade produced more accurate estimates than the results obtained before in [28, 30].

1.3 Thesis Contribution

The two different solutions to the problem of mass and grade estimation described above have been promising when evaluated with two sets of experimental data obtained in 2002 on Interstate 15 north of San Diego by Vahidi and his colleagues. However there were still several issues that required further investigation before the algorithms could be implemented reliably and robustly in a vehicle. Therefore over the course of this master thesis research, we have worked closely with Eaton Corporation's Research and Development Group to refine and improve these existing algorithms and to extend their use to a wider range of operating conditions. In particular we have researched methods for minimizing the influence of gear shift, clutch disengagement, braking, and lack of excitations at low velocities on the estimation results. Along this path we have performed analysis and comparative studies to determine where and which of the algorithms is strongest and where they need further development. The fixes we have proposed have improved the estimators in a number of areas in particular during critical gear shift period. For the first algorithm we have selected a suitable filter for removing noise and the forgetting factors that give consistent results over a number of data sets. With the refinements made, the only major remaining issue of algorithm I ("Recursive Least Square with Multiple Forgetting") is its

sensitivity to initialization which influences the mass estimate. We have verified that algorithm II ("Two Stage Lyapunov-Based Nonlinear Estimator") does not face this issue and therefore can be the solution to initialization. Another strength of algorithm II validated with Eaton data is its more robust convergence to the actual values of grade. The main issues with second algorithm were related to the speed of convergence and to reduce the computation time to make algorithm feasible to implement in real time. We have resolved several of these issues and the fixes for the same are explained in chapter 5 in detail.

Development and verification of the vehicle longitudinal dynamics model and the first proposed methodology, RLS with multiple forgetting, are described in Chapter 2. In Chapter 3 we explain the changes made in the original algorithm and the results obtained for different sets of experimental data provided by Eaton. We also describe the remaining issues to be addressed in the future. Chapter 4 outlines the second two-stage estimation algorithm; and chapter 5 summarizes the results obtained using this second algorithm to this date. The conclusions also outline directions for future research.

Chapter 2

Algorithm I: Recursive Least Square with Multiple Forgetting

The proposed estimation approach is a model-based scheme; it uses a model of vehicle longitudinal dynamics and signals available from vehicle Control Area Network to estimate the vehicle acceleration. The difference between the estimated acceleration and measured acceleration drives the estimator for mass and grade. The vehicle longitudinal dynamics model is laid out next followed by the least square estimation strategy.

2.1 Vehicle Longitudinal Dynamics

The vehicle longitudinal dynamics equation is simply described by Newton's second law of motion. The vehicle acceleration is a result of traction produced by the engine and resistive forces due to braking, aerodynamic drag, rolling resistance, and road grade. Here we assume that the wheels do not slip and the vehicle travels on a straight path. It is also assumed that all engine torque is passed to the wheels when the clutch is fully engaged. With these assumptions longitudinal dynamics of vehicle can be presented in the following

simple form,

$$M\dot{v} = \frac{T_e - J_e\dot{\omega}}{r_g} - F_{fb} - F_{aero} - F_{grade} \tag{2.1}$$

In this equation M is the total mass of the vehicle, v is the velocity of the vehicle and ω is the engine's rotational speed. The net engine output torque is T_e. The engine torque is positive when engine is in fueling mode, it can be negative when fuel is cut or when compression braking is activated[1] The combined powertrain inertia is reflected in J_e and the term $J_e\dot{\omega}$ in equation (2.1) represents the portion of torque spent on rotating the powertrain. We define r_g as the ratio of wheel radius to total gear ratio,

$$r_g = \frac{r_w}{g_d g_f}$$

where r_w is the wheel radius, g_d is the gear ratio and g_f is the final driveline ratio. The braking force generated at the wheel while braking is F_{fb}, and the aerodynamic drag force is given by,

$$F_{aero} = \frac{1}{2} C_d \rho A v^2$$

where C_d is the drag coefficient, ρ is a mass density of air and A is frontal area of the vehicle. F_{grade} represents the combined force due to road grade and rolling resistance of the road. It can be defined as,

$$F_{grade} = Mg(\mu\cos\beta + \sin\beta),$$

where g is the gravity constant. In this equation β represents road grade where $\beta = 0$ represents no inclination, positive β corresponds to uphill grade, and negative β corresponds to downhill grade.

[1] In the experimental results provided by Eaton, the engine compression braking mode was never activated.

Equation (2.1) can be rearranged to separate vehicle mass and road grade in two different terms. After rearranging equation (2.1) can be written as,

$$\dot{v} = (\frac{T_e - J_e\dot{\omega}}{r_g} - F_{fb} - F_{aero})\frac{1}{M} - \frac{g}{\cos(\beta_\mu)}\sin(\beta + \beta_\mu) \tag{2.2}$$

where $\tan(\beta_\mu) = \mu$. We can rewrite Eq. (2.2) in the following form,

$$y = \phi^T\theta,\ \phi = [\phi_1, \phi_2]^T\ \theta = [\theta_1, \theta_2]^T \tag{2.3}$$

where

$$\theta = [\theta_1, \theta_2]^T = [\frac{1}{M},\ \sin(\beta + \beta_\mu)]^T$$

are the unknown parameters of the model, which we try to estimate and

$$y = \dot{v},\ \phi_1 = \frac{T_e - J_e\dot{\omega}}{r_g} - F_{fb} - F_{aero},\ \phi_2 = -\frac{g}{\cos(\beta_\mu)}$$

can be calculated based on measured signals and known variables.

Had the parameters θ_1 and θ_2 been constant, a simple recursive algorithm, like recursive least squares, could have been used for estimation. However while θ_1 depends only on mass and is constant, the parameter θ_2 is in general time-varying.

2.1.1 Calculation of Model Parameters

In the vehicle longitudinal dynamics equation (2.2), the wheel radius r_w, driveline inertia J_e, drag coefficient C_d, and coefficient of rolling resistance μ, are unknown and should be determined before the model can be used for estimation of mass and grade.

The value for tire rolling radius, $r_w = 20$inch was provided by Eaton Trucks. We fixed the coefficient of rolling resistance to 0.008 and drag coefficient to 0.65. A range for

these values was provided to us by our industrial collaborator at Eaton. The values have been fine-tuned such that the simulated acceleration matched the actual acceleration of the truck closely. In the model we have assumed that velocity and engine speed are always proportionally related and that transmission is always engaged. These assumptions do not hold during gearshift periods due to interruption in flow of power to the wheels. However this only results in local mismatch between the model outcomes and experimental results and in general the model represents the longitudinal dynamics adequately well.

Having identified a model of the vehicle longitudinal dynamics, we continue with the theory of RLS estimation and the estimated algorithm.

2.2 Recursive Least Square Estimation

In least square estimation strategy the unknown parameters θ, are selected in such a way that the sum of the square of the difference (error) of observed and estimated value is minimized [1]. With the longitudinal dynamics equation represented in (2.2), we seek the estimate $\hat{\theta}$ that minimize the following function,

$$V(\hat{\theta}, n) = \frac{1}{2} \sum_{i=1}^{n} \left(y(i) - \phi^T(i)\hat{\theta} \right)^2 \tag{2.4}$$

The closed-loop solution for (2.4) is,

$$\hat{\theta} = \left(\sum_{i=1}^{n} \phi(i)\phi^T(i) \right)^{-1} \left(\sum_{i=1}^{n} \phi(i) y(i) \right) \tag{2.5}$$

In this problem we are interested in real-time implementation of the estimation scheme, so it is more appropriate to update the estimates recursively. The recursive update

law for least-square is standard and can be written as,

$$\hat{\theta}(k) = \hat{\theta}(k-1) + L(k)\left(y(k) - \phi^T(k)\hat{\theta}(k-1)\right) \tag{2.6}$$

where

$$L(k) = P(k)\phi(k) = P(k-1)\phi(k)\left(1 + \phi^T(k)P(k-1)\phi(k)\right)^{-1} \tag{2.7}$$

and

$$P(k) = \left(I - L(k)\phi^T(k)\right)P(k-1) \tag{2.8}$$

Here $P(k)$ is referred to as covariance matrix. Equation (2.6) updates the the parameter estimation in each step based on the difference between measured and estimated signal. In most recursive estimation schemes the basic form of equation is similar to (2.6); the only difference is how the gain $L(k)$ is updated.

2.2.1 Recursive Least Square Estimation with Forgetting

When the unknown parameters are expected to remain constant, a simple RLS method as described above can be used for parameter estimation. However when the unknown parameters are time-varying, the standard RLS approach is not suitable. Two different heuristic approaches have been traditionally used to handle time-varying parameters[1]: i) In a covariance-resetting approach the covariance matrix P is reset periodically to ensure the estimator remains sensitive to the new data received. ii) In another approach the estimation error is penalized by a "forgetting factor" which gives the recent data more weight than older data. As a result the older information is gradually "forgotten" in favor of newer information and a change in parameter values may be detected. The modified cost function

for "RLS with forgetting" is,

$$V(\hat{\theta},k) = \frac{1}{2}\sum_{i=1}^{k} \lambda^{k-i}\left(y(i) - \phi^T(i)\hat{\theta}(k)\right)^2 \tag{2.9}$$

where λ is called the forgetting factor and $\lambda \in [0,1]$. The forgetting factor operates as a weight which diminishes for the older data. The scheme is known as least-square with exponential forgetting and θ can be calculated recursively using the same update equation (2.6) but with $L(k)$ and $P(k)$ derived as follows:

$$L(k) = P(k-1)\phi(k)\left(\lambda + \phi^T(k)P(k-1)\phi(k)\right)^{-1} \tag{2.10}$$

and

$$P(k) = \left(I - L(k)\phi^T(k)\right)P(k-1)\frac{1}{\lambda}. \tag{2.11}$$

The main difference between simple RLS method and and RLS with forgetting is how the covariance matrix $P(k)$ is updated with each sample. In classical RLS method the covariance matrix $P(k)$ goes to zero with time losing the sensitivity to new data. Where as in RLS with forgetting factor, in each step the covariance matrix $P(k)$ is divided by the forgetting factor $\lambda < 1$ and therefore is kept "alive" (2.11). This keeps the estimator more sensitive to parameter variation and is proven to converge, under certain persistence of excitation conditions, and when the unknown parameters reach a constant value [6], [13].

The RLS with forgetting is widely used in many engineering applications to estimate time-varying parameters. Like any other estimation scheme existence of persistent excitation is key to successful estimation. For RLS with forgetting specifically, lack of excitation may lead to covariance wind-up resulting in poor estimation or blow-up. This problem has been addressed by many researchers and many different solutions have been proposed. Author of [10] has proposed time-varying forgetting factor, in which during low

excitation higher forgetting factor (closer to unity) is selected. The scheme proposed in [25] suggests turning off the estimator during period of low excitation along with a time-varying forgetting factor. Resetting the covariance matrix during low excitation is proposed in [23]. The concept of "directional forgetting" is also proposed as a fix in various publications including [11], [14], [7], [5].

The estimator windup may also occur when estimating multiple parameters that vary at different rates. In the mass and grade estimation problem, the vehicle mass remains constant in one trip while road grade can vary continuously. Vahidi et al. show in [30] that RLS with a single forgetting factor fails to generate reliable estimates for both mass and road grade. In the literature strategies such as RLS with vector forgetting [21], [22] and selective forgetting [19] are proposed to handle different rates of parameter variation.

In RLS with vector forgetting, the covariance matrix is scaled by a diagonal matrix of different forgetting factors instead of dividing the covariance matrix by single forgetting factor,

$$P(k) = \Lambda^{-1}\left(I - L(k)\phi^T(k)\right)P(k-1)\Lambda^{-1} \tag{2.12}$$

where

$$\Lambda = diag[\lambda_1, \lambda_2, \ldots, \lambda_n]$$

is a diagonal matrix of different forgetting factors each corresponding to one unknown parameter. This method, although heuristic, has proved effective in estimating multiple parameters which vary at different rates (see for example [34]).

In [27] a method similar to vector-type forgetting for estimation of vehicle mass and road grade is proposed. This method has been promising in estimating a constant vehicle mass and slowly-varying road grade when tested with experimental data. This is one of the two algorithms that are further refined in this master thesis and therefore is summarized next.

2.2.2 Recursive Least Square with Multiple Forgetting

In RLS with multiple forgetting proposed in [27] the estimation cost function is broken in two parts allowing use of different forgetting factors for each parameter,

$$V(\hat{\theta}_1(k),\hat{\theta}_2(k),k) = \frac{1}{2}\sum_{i=1}^{k}\lambda_1^{k-i}\left(y(i)-\phi_1(i)\hat{\theta}_1(k)-\phi_2(i)\theta_2(i)\right)^2 + \frac{1}{2}\sum_{i=1}^{k}\lambda_2^{k-i}\left(y(i)-\phi_1(i)\theta_1(i)-\phi_2(i)\hat{\theta}_2(k)\right)^2. \quad (2.13)$$

With this definition for the loss function the first term on the right hand side of equation (2.13) represents the error of the step k due to first parameter $\hat{\theta}_1(k)$ and the second term corresponds to the error due to second parameter $\hat{\theta}_2(k)$. Here λ_1 and λ_2 are the forgetting factors for first and second parameters respectively. Use of multiple forgetting factors provides more degrees of freedom for tuning the estimator. After some manipulation the final form of this recursive estimator is given in [27] as follows,

$$\hat{\theta}(k) = \hat{\theta}(k-1) + L_{new}(k)\left(y(k)-\phi^T(k)\hat{\theta}(k-1)\right) \quad (2.14)$$

where $L_{new}(k)$ is defined as follows:

$$L_{new}(k) = \frac{1}{1+\frac{P_1(k-1)\phi_1(k)^2}{\lambda_1}+\frac{P_2(k-1)\phi_2(k)^2}{\lambda_2}}\begin{bmatrix}\frac{P_1(k-1)\phi_1(k)}{\lambda_1}\\ \frac{P_2(k-1)\phi_2(k)}{\lambda_2}\end{bmatrix} \quad (2.15)$$

and the covariance matrix is now decoupled into P_1 and P_2 each recursively obtained by,

$$P_1(k) = \left(I-L_1(k)\phi_1^T(k)\right)P_1(k-1)\frac{1}{\lambda_1}$$

$$P_2(k) = \left(I-L_2(k)\phi_2^T(k)\right)P_2(k-1)\frac{1}{\lambda_2}$$

The RLS with multiple forgetting described above is referred to as algorithm I in the rest of this thesis. In the next chapter modifications are proposed that improves the robustness and applicability of the method. Experimental data are used to test the algorithm.

Direct implementation of (2.2) in least square estimation requires differentiation of velocity and engine speed signals. Differentiation of velocity will magnify the velocity noise to much higher values and the differentiated data may not be useable. In [27] to circumvent this problem, it is proposed to integrate both sides of (2.2) over time and apply the estimation scheme to the new formulation. We adopt the same methodology in our implementation of Algorithm I.

Chapter 3

Refinement of Algorithm I and Results

This section explains the modifications made to Algorithm I and demonstrates the performance using experimental data. We have used three different data sets to verify this algorithm. After a brief description of the experimental data sets and measured signals, and validation of vehicle longitudinal dynamics, the performance of the estimator with experimental data are shown.

3.1 The Road Profiles

Algorithm I was tested using three sets of data provided by Eaton. The data sets are referred as data set 1, 2 and 3. The road profiles of all three runs are shown in Figures 3.1, 3.2, and 3.3.

3.2 Measured Signals

Many signals required for estimation are available through vehicle Control Area Network (CAN). Most of these signals are communicated based on the SAE J1939 proto-

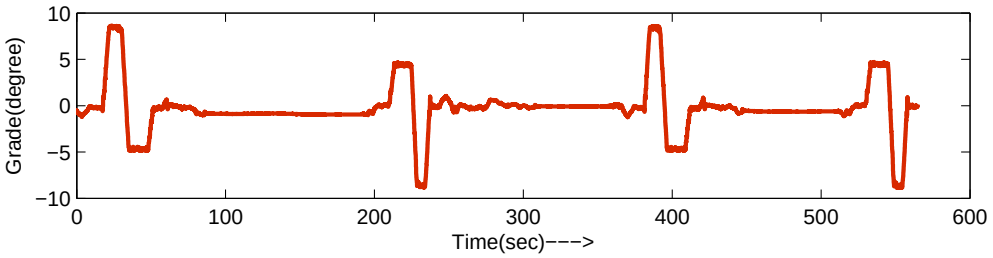

Figure 3.1: Data set-1 grade profile.

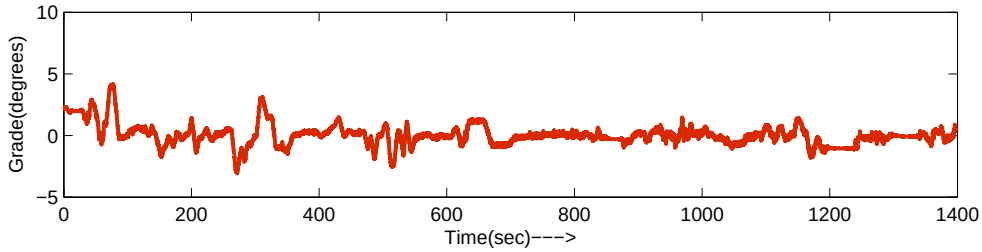

Figure 3.2: Data set-2 grade profile.

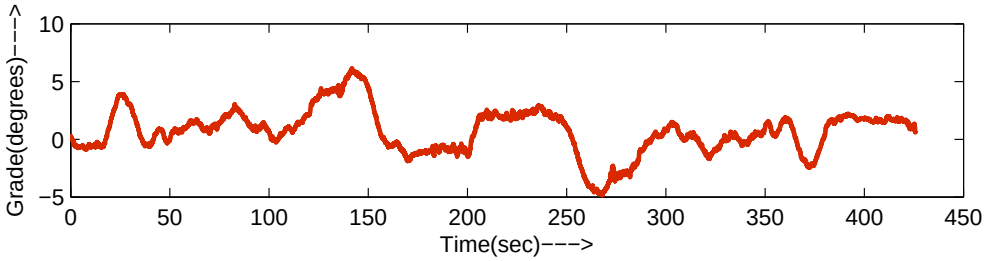

Figure 3.3: Data set-3 grade profile.

col, the standard for heavy duty vehicles. There were also data coming from a number of sensors including a torque sensor mounted on the vehicle drivetrain.

Accelerator pedal signal(0 to 100), brake pedal signal, clutch engagement signal, current gear number, selected gear number, net engine output torque, retarded torque, gear shift state are the signals available from the CAN of the vehicle. Torque on the final drive-line is measured using a customized sensor. Pitch angle, forward velocity and acceleration, altitude, etc. signals are available from GPS. All signals are sampled at 0.01 second.

3.3 Signal Filtering

In a real scenario the situation can become more challenging due to higher level of uncertainties. The signals are potentially delayed and many times the signals are noisy and biased in one direction rather than being only affected by pure white noise. Moreover, the delay or noise level in one signal is normally different from the other signals. However use of low-pass filters with the same cut-off frequency seemed accurate for the purpose of mass and grade estimation. To reduce the noise and hence the oscillations in the measured signals we have filtered the (1) engine torque, (2) velocity, and (3) estimated grade using Butterworth filters. In particular we have used a second-order low-pass Butterworth filter with cutoff frequency of 0.5 Hz to filter the engine torque and velocity signals. Moreover to reduce the noise level in the estimated grade, we have used a second-order low-pass Butterworth filter with cutoff frequency of 0.8 Hz.

3.4 Refinement and Validation of the Vehicle Model

The longitudinal vehicle dynamics model given in equation (2.2) assumes a clutch that is always engaged, a perfect gear shift process and knowledge of all the forces including the braking force F_{fb}. These assumptions are not valid during the gearshift period when the clutch is disengaged. Also in a standard setting the service brake pressure and subsequently the torques cannot be accurately determined. Developing an accurate model of the transmission and the gear shift process is an option but overcomplicates the model used for estimation; therefore we employed a simple but effective approach to model the flow of torque during shifting: When the shift state is 1 (complete engagement) the driveline torque is obtained by multiplying the engine torque by the gear ratio; and when the shift state is 5 (complete clutch disengagement); the driveline torque is assumed to be zero. Because the applied brake forces are not known, we have tuned and determined fixed brake pressures that cause the modelel velocity match the measured velocity. Figures 3.4, 3.5, and 3.6

show the modeled velocity versus measured velocity, for all three data sets. Figure 3.4 shows good agreement between the measured and modeled velocities for the data set-1 where the uncertainties in the road profile is minimal. Slight differences between the model and actual velocity in this figure can be attributed to periods of gear shift or braking and the approximations we made in the model. In some portions of Figures 3.5 and 3.6 the discrepancies between the model and actual velocity are larger which may be due to inaccurate road grade assumptions. Because the data set-1 seems more reliable we base most of our estimation analysis on this set of data.

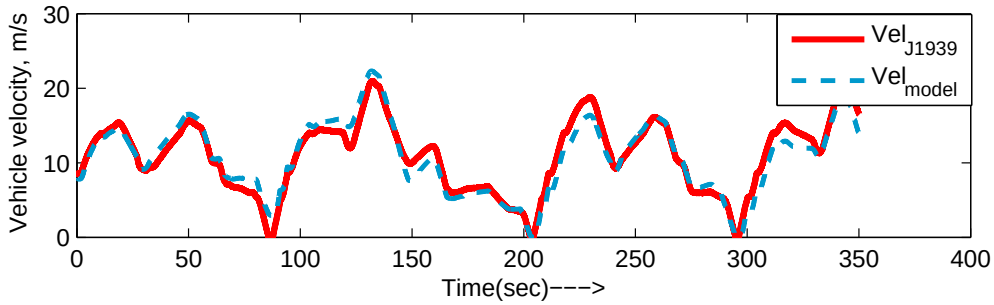

Figure 3.4: Comparison of model velocity and measured velocity - data set-1

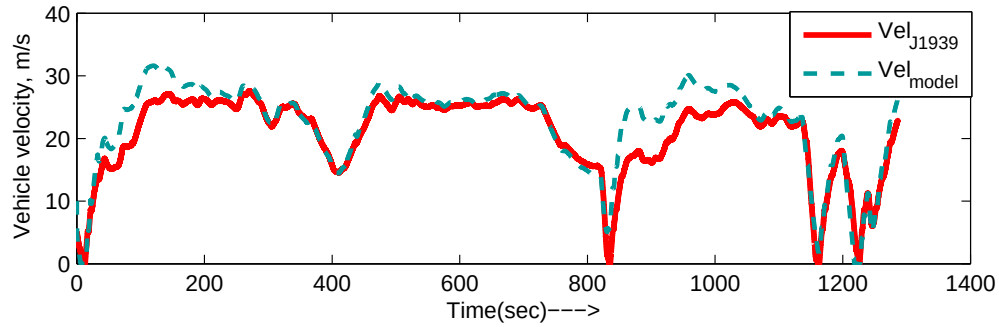

Figure 3.5: Comparison of model velocity and measured velocity - data set-2

Eaton had also provided a torque sensor reading on the final drive. To ensure validity of the gear shift model we have compared the final-drive torque, as measured by the torque sensor, to the the engine torque reflected on the final driveline;

$$T_{finaldrive} = T_{engine} \times \text{Gear Ratio} \times \text{Clutch State} \times \text{Driveline Efficiency}$$

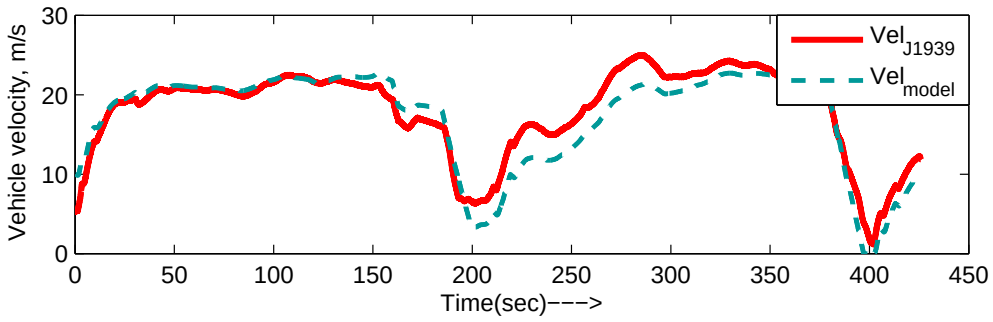

Figure 3.6: Comparison of model velocity and measured velocity - data set-3

and have shown the results in Figure 3.7. There is a close correspondence between torque sensor reading and calculated torque from engine.

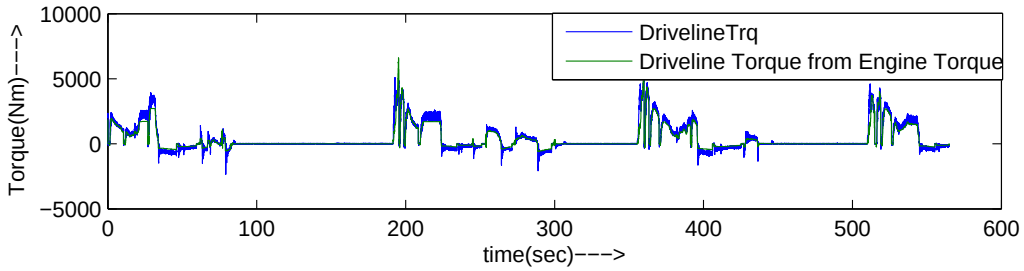

Figure 3.7: Comparison of sensor torque and engine torque when reflected on final driveline

With the accuracy of the model tested, the next section describes the results obtained with the original version of algorithm I.

3.5 Results With Algorithm-I

The estimation is initialized in a batch mode to obtain an initial estimate of mass and road grade. During the batch period, which does not last more than a few seconds, we assume the unknown mass and grade are constant and use a standard least-square algorithm to find a constant estimate for mass and grade. Good initial estimates are obtained only when the chosen batch is rich in excitations. Therefore it is critical to initialize the estimator

in a period when sufficient excitations are present. Once an initial estimate of mass and grade is obtained; the algorithm switches to its recursive mode for which the recursive least square with multiple forgetting factors described in Chapter 2 is used.

We first apply the algorithm I in its original form to data set-1. The results are shown in the Figure 3.8. The estimation starts around the recorded time of 60 seconds from when the truck starts moving. The initial batch size included 200 sampling intervals, that is 2 seconds with the sampling time of 0.01 seconds. The recursive scheme kicks in next; the forgetting factors for mass and grade are chosen to be 0.95 and 0.5 respectively to reflect a constant mass and time-varying road grade. The first plot in Figure 3.8 compares the estimated road grade to the actual grade. The second subplot in figure 3.8 shows the mass estimate and Figure 3.9 shows the percentage error in the mass estimate. As shown in the figure the maximum percent mass error after 250 seconds is around 10%. Figure 3.10 superimposes the clutch engagement signal on the grade estimate, showing a correspondence between shift periods and intervals when the grade estimate is poor. The main difficulty seen in the above estimation results is the sporadic spikes in the grade estimates which are believed to be triggered by the gear shift process. The reason could be due to unmodeled shift dynamics and/or vibrations caused by the shift process. Also part of the data included periods when the truck was stopped (between 100 and 200 seconds for example) during which the mass estimate deviates from the actual value; this is due to lack of excitations at zero velocity. We dedicated a big part of our effort to understanding and providing a solution to these problems. Next section summarizes the final results.

3.5.1 Adjustments to Algorithm I

During periods of low excitations, in particular when the vehicle is stopped, the estimator is not receiving persistently exciting data and therefore it should be turned off. To remedy this problem, as a first fix, periods of zero velocity are detected and omitted from

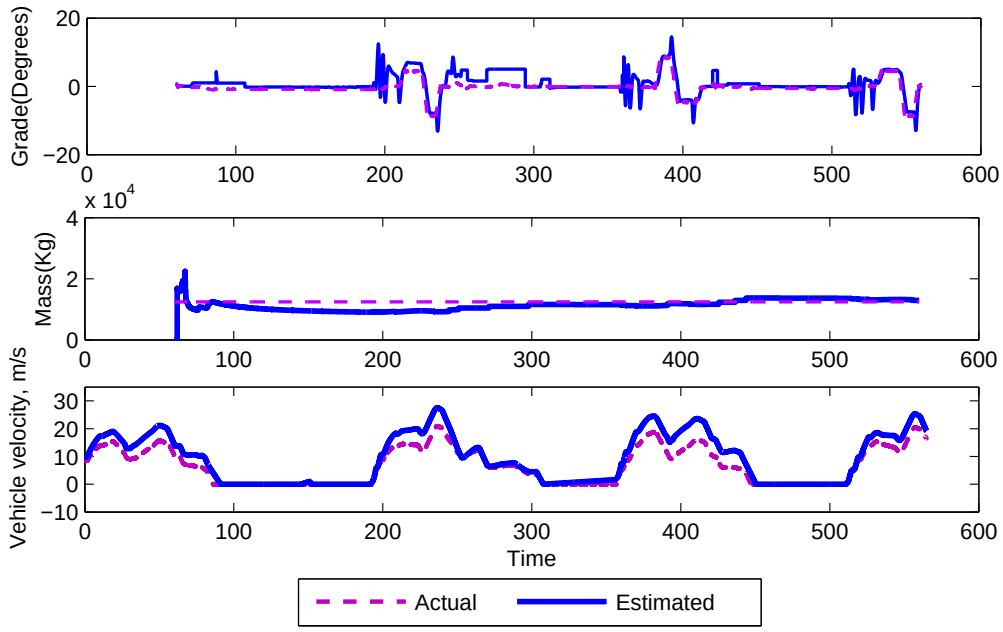

Figure 3.8: Estimated road grade and mass using algorithm I for data set-1(batch size= 200, forgetting factor for grade= 0.5 and for mass= 0.95)

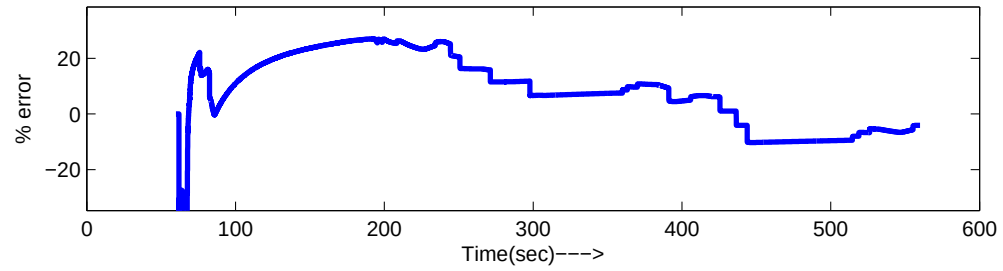

Figure 3.9: Percent mass error for data set-1; (batch size=200, forgetting factor for grade = 0.5 and for mass = 0.95)

the data fed to the estimator. Therefore in the forthcoming results stopping periods are not included in the plots. Another major problem is the spiky grade estimate during the gearshift periods. Because including an accurate dynamic shifting model complicates the estimation, we decided to stop the estimator when shift is in progress and turn it back on when the shift is complete. During these periods the mass and grade estimates are taken as their latest calculated values. Since the gearshift period is on the order of a second; this approximation should not have a large influence

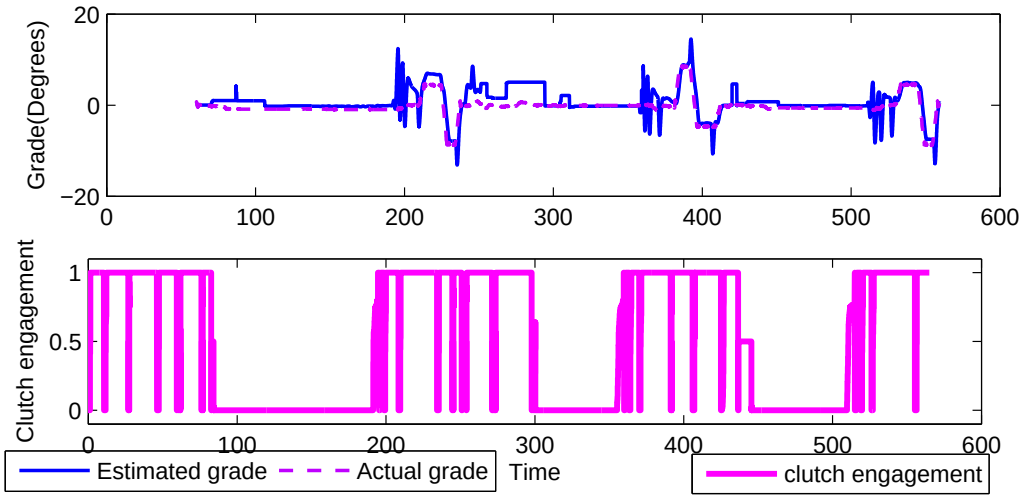

Figure 3.10: Comparison of estimated grade with clutch engagement signal

on the applications that use mass and grade estimates. The performance of algorithm I with this fix was tested and improvements in grade estimates were observed.

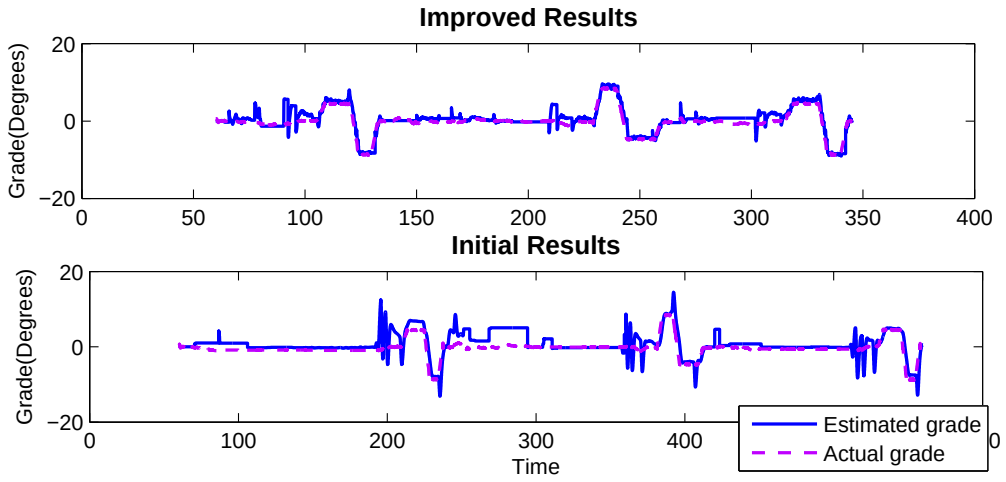

Figure 3.11: Estimated road grade with the fixes to the algorithm using data set-1. (batch size=390, forgetting factor for grade = 0.6 and for mass = 0.9).

However even after full engagement of the clutch, the grade estimates had occasional spikes. The drivetrain vibration subsequent to clutch engagement may be the cause of this problem. To reduce the spikes in grade estimate, we decided to discard the estimated values of mass and grade for an additional 40 sampling times (0.4 seconds) after clutch engagement and report the latest

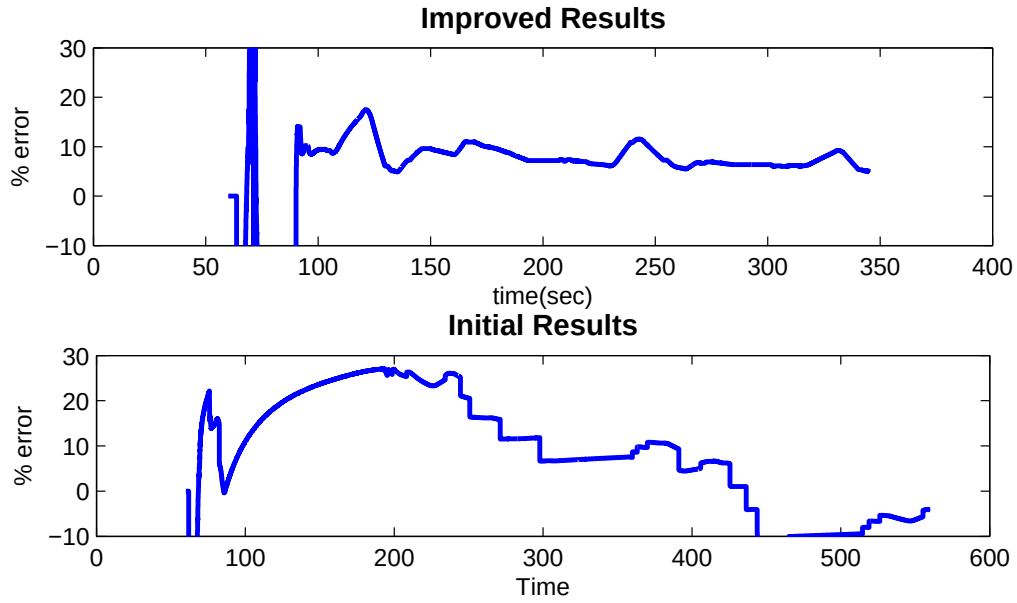

Figure 3.12: Percent mass error with the fixes to the algorithm using data set-1. (batch size=390, forgetting factor for grade = 0.6 and for mass = 0.9).

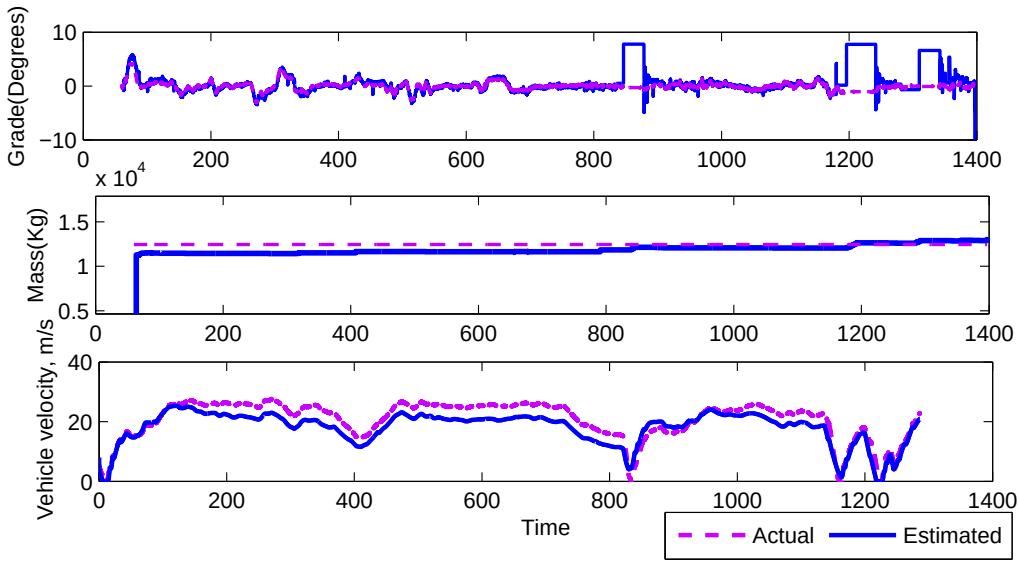

Figure 3.13: Estimated road grade and mass with the fixes to the algorithm using data set-2. (batch size=390, forgetting factor for grade = 0.2 and for mass = 0.98).

estimates obtained before the shift started (note that the estimator is turned back on right after the clutch is engaged). When the brakes are applied a constant brake pressure, determined from the

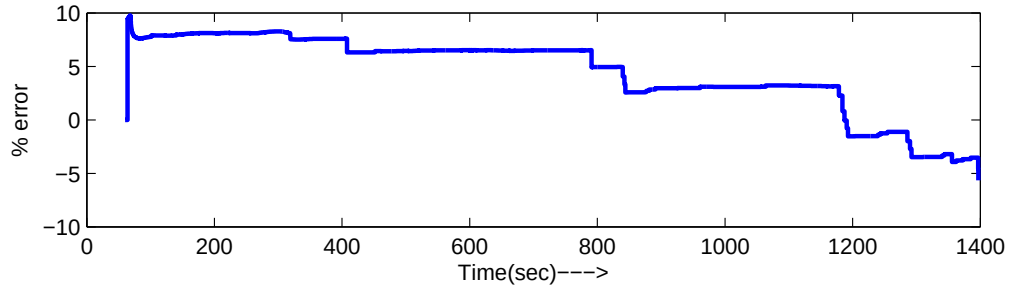

Figure 3.14: Percent mass error with the fixes to the algorithm using data set-2. (batch size=390, forgetting factor for grade = 0.2 and for mass = 0.98).

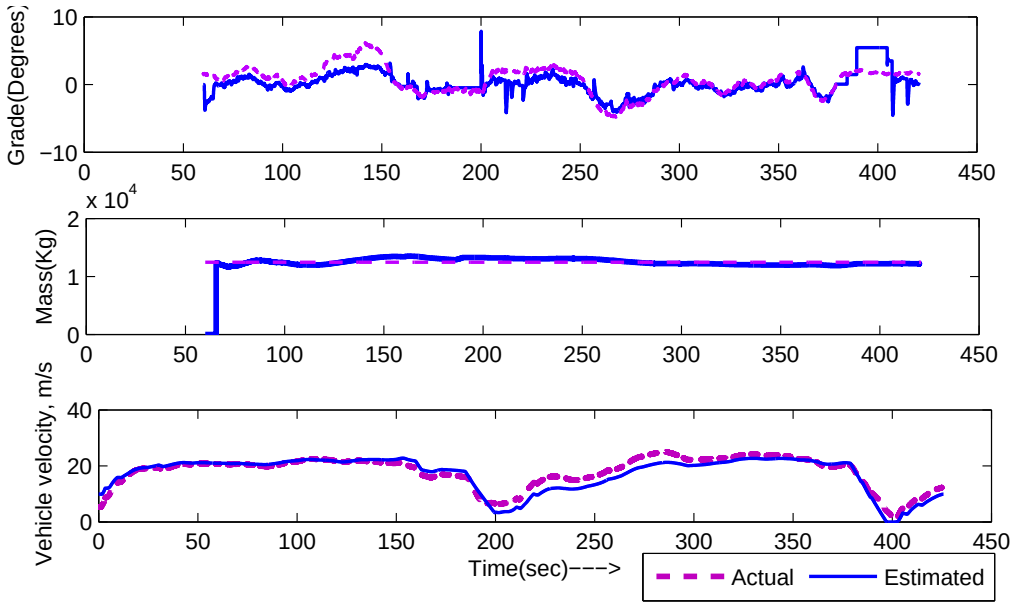

Figure 3.15: Estimated road grade and mass with the fixes to the algorithm using data set-3. (batch size=550, forgetting factor for grade = 0.6 and for mass = 0.9).

model validation stage, is assumed. While the estimator continues to run during the braking period; we discard its estimates and report the latest estimate obtained before the application of brakes. This helps improve the estimation outcomes.

Figures 3.11 and 3.12 show the performance of the estimator with these additional fixes for data set-1. In these figures the vehicle stop time data are removed and therefore the time plots are shorter than those reported in the last section. It can be seen that the grade estimate has significantly improved over the results shown in Figures 3.8 and 3.9. The mass estimate also improves and

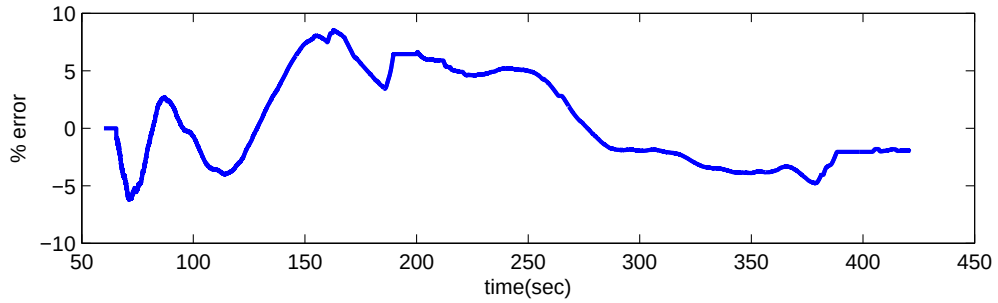

Figure 3.16: Percent mass error with the fixes to the algorithm using data set-3. (batch size=550, forgetting factor for grade = 0.6 and for mass = 0.9).

reaches within 8% of its actual value at the end of the run. The remaining spikes at or around $t = 100$ second are believed to be due to the mass estimate which is not accurate at this initial stage.

The same process is repeated using the remaining two data sets and results are shown in Figures 3.13, 3.14,3.15, and 3.16. The grade estimates for both cases are accurate for most part of the run and follow the actual grade profile closely except when there is a gear-shift. Also the mass estimates for both cases are within 10% of the actual mass. We tried to get the results using the same setup as we used for data set-1 (e.g. same forgetting factors, same batch size); with those we do not necessarily get the best results. Therefore for data set-2 we have used forgetting factor for mass and grade as 0.98 and 0.2 respectively and batch size of 390(same as used for data set-1), and for data set-3 we have used 0.9 and 0.6 as mass and grade forgetting factors respectively and batch size of 550. The robustness to the choice of forgetting factors and batch size is listed as one of the future steps for improving algorithm I.

Table 3.1 shows and compares the estimation result qualitatively when the same setup is used for the estimator (same batch size and forgetting factors) for all sets of data. Three different batch sizes and four different sets of forgetting factors were used for all sets of data. In the table we have displayed the percent error in mass at the end of the cycle for each case and grade estimate is rated only qualitatively as good or poor. The percent error for grade would not be meaningful because the actual grade for most part of the run is zero or close to zero, making the percent error meaningless.

Table 3.1: Results for all sets of data using different batch size and forgetting factors

Batch Size	Forgetting Factor		Data set-1		Data set-3		Data set-3	
	For Mass	For Grade	% mass error	Grade	% mass error	Grade	% mass error	Grade
370	0.9	0.6	5	good	26	good	58	poor
	0.8	0.6	7.5	good	32	poor	38	poor
	0.8	0.7	6.5	poor	36	poor	30	poor
	0.98	0.2	55	poor	39	poor	5	good
450	0.9	0.6	9	good	32	good	63	poor
	0.8	0.6	15	good	30	good	39	poor
	0.8	0.7	10	good	28	good	36	poor
	0.98	0.2	45	poor	34	good	21	good
550	0.9	0.6	20	poor	3	good	65	poor
	0.8	0.6	1	good	70	poor	43	poor
	0.8	0.7	1.5	good	60	bad	30	poor
	0.98	0.2	60	poor	80	poor	28	poor

3.5.2 Extended Simulation Results

To investigate the performance of the estimator over longer time, the simulations were ran over an extended set of data. We created a new data set by augmenting the data set-1 back-to-back. Figures 3.17 and 3.18 show the results of an extended simulation with the data set-1 repeated twice. The results indicate that the estimator remains robust when running for longer times. Figure 3.19 superimposes the grade estimates from the two simulation cycles for better comparison. From this figure there does not seem to be a major improvement in grade estimates when the estimator runs longer. We also ran the estimator for five cycles to further investigate the convergence of estimated valued over the time; while the mass estimate converged further, the remaining spikes in the estimated grade are not significantly reduced over time.

3.6 Future Research For Algorithm I

While the performance of algorithm I is further scrutinized and subsequently improved, there is still room for improvement in several areas.

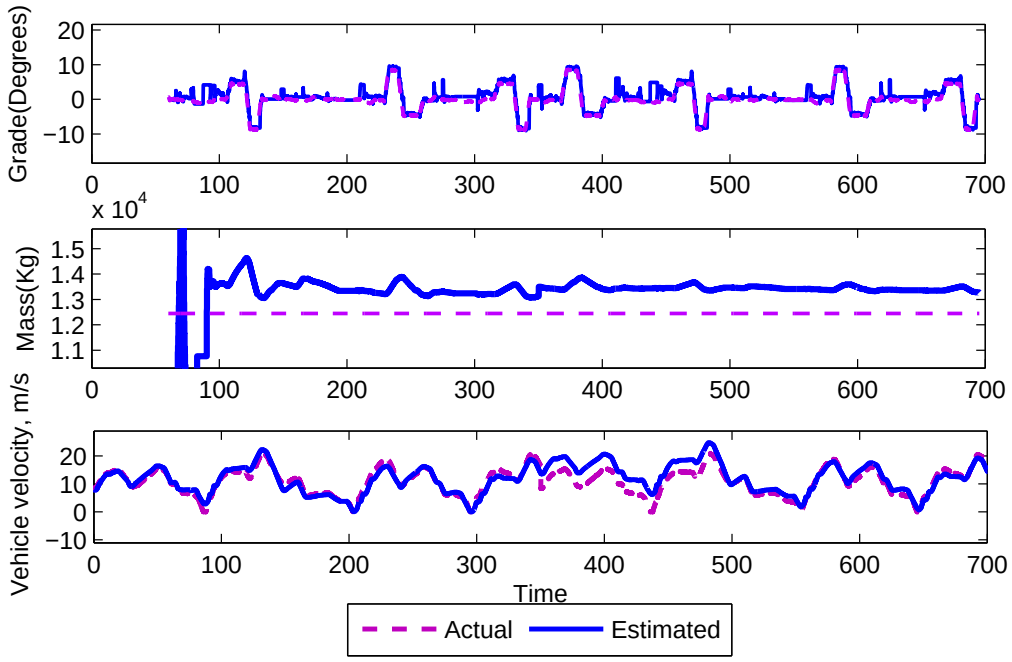

Figure 3.17: Estimated road grade and mass in an extended run (batch size=390, forgetting factor for grade = 0.6 and for mass = 0.9)

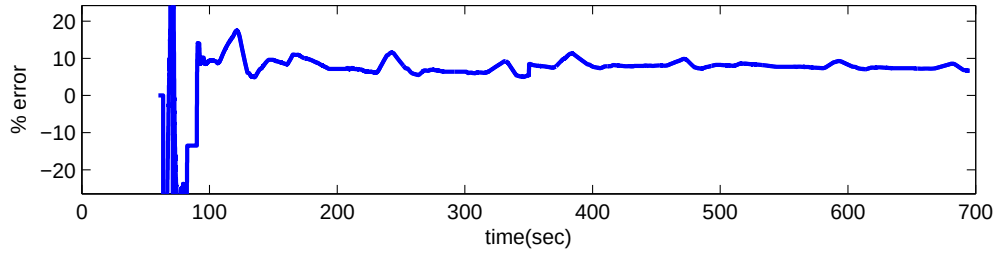

Figure 3.18: Percent mass error in an extended run (batch size=390, forgetting factor for grade = 0.6 and for mass = 0.9)

3.6.1 Adaptive Batch Sizing

The main bottleneck to the performance of algorithm I is selection of a suitable batch size which determines the initial estimates and influences the rest of the recursive estimation procedure. While for each set of data we have been able to determine a batch size that results in acceptable initialization, the best batch size has often deferred between various data sets. For example when data set-1 was used a batch size of 390 sample provided better results and in the case of data set-3 a

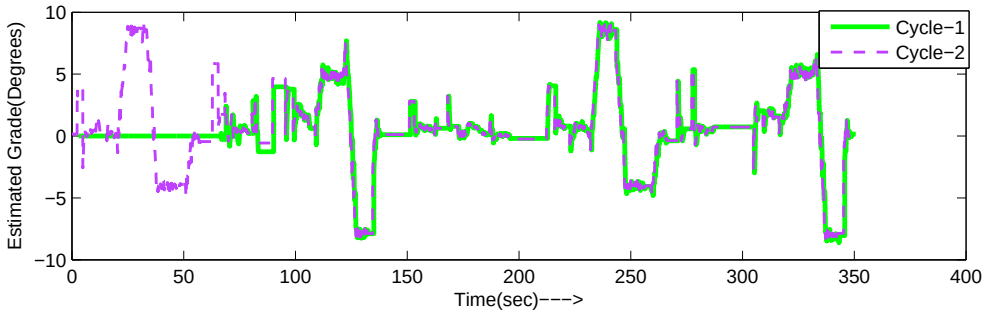

Figure 3.19: Comparison of grade estimated over two cycles of data set-1 (batch size=390, Forgetting factor for grade = 0.6 and for mass = 0.9)

batch of 550 samples. We believe this difference could be attributed to different levels of excitations available in each set of data. Before the algorithm can be implemented in production, it is important to devise a methodology that detects the level of signal excitation and intelligently selects an appropriate batch size. One method would be to check an index attributed to the persistence excitation and continue the batch estimation up to when the persistent excitation is above the particular limit. To ensure the sufficient excitation level we can use the following condition:

$$\sum_{i=1}^{N} \phi(i)\phi(i)^T > \rho \times I_{(2\times 2)}$$

where ϕ is the regressor vector at each time and ρ is a threshold indicating level of excitation.

A different approach would be devising a logic that depicts the right portions of data that makes up a rich batch. For example an algorithm can be devised to detect periods of large acceleration but with minimum gear shift which is believed to be a good batch candidate and should result in more accurate estimates of mass.

3.6.2 Forgetting Factors

While the algorithm is not as sensitive to a reasonable variation in forgetting factors, still the quality of the estimates depends on the choice of forgetting factors. For example for data set-1 and data set-3 we have used forgetting factor for mass = 0.9 and for grade = 0.6. The same

forgetting factors for data set-2, did not generate the possible estimates. Instead for data set-2 the forgetting factors of 0.98 for mass and 0.2 for grade generated better results. This might be due to lower quality of signals as compared to the two other set of data; however further investigation is necessary before implementation. Use of a time-varying forgetting factor has been proposed in the past for estimating a single time-varying parameter using RLS with single forgetting [10] and is known to improve the estimation results. This is another area which warrants investigation, as so far we have always used fixed forgetting factors.

3.6.3 Issues During Gear-shift

As mentioned previously, the original algorithm was designed with the assumption that there is no gear-shift during the run. So, there were spikes in the estimated grade during the shift when the original algorithm was employed. To overcome these spikes we turned the estimator off when the clutch was not fully engaged which significantly improved the quality of estimation. However there still remain some spikes in the grade estimates. It is important to more closely examine these occurrences and determine the cause. A challenging but worthwhile future track is to develop a more accurate model of the transmission and integrate it effectively with the vehicle longitudinal dynamics model. To the best of our knowledge this has not been done in the past for the purpose of vehicle parameter estimation.

3.6.4 Covariance Resetting

A well-known problem with a recursive least-square algorithm is the fact that the estimator covariance diminishes to zero quickly and as a result the estimator loses sensitivity to new measurements. This is not a desirable effect when we wish to track time-varying parameters. In fact, the benefit of forgetting factors is their influence on magnifying the covariance matrix. Another valid approach proposed in the estimation literature is to reset the covariance matrix periodically so that the estimator remains sensitive to variation in parameter values. This could be one more promising direction for improving the performance of algorithm I.

Chapter 4

Algorithm II: The Two-Stage Nonlinear Estimator

The second algorithm shown here is a two-stage approach for estimation of vehicle mass and time-varying road grade. The first stage of this algorithm is a least square estimator which determines estimates of the vehicle mass and constant grade, based on the longitudinal dynamics of the vehicle. Because the road grade is time-varying, in the second stage a nonlinear estimator [20, 2] based on Lyapunove method is used which provides more accurate estimate of road grade. In this estimation scheme, the mass of the vehicle is determined using adaptive least square method [28, 30] and estimated mass in the first stage is utilized in the 2nd stage to estimate the road grade[1].

4.1 Longitudinal Dynamics of the Vehicle

The vehicle longitudinal dynamics model developed before in equation (2.2) is used here as well,

$$\dot{v} = (\frac{T_e - J_e\dot{\omega}}{r_g} - F_{fb} - F_{aero})\frac{1}{M} - \frac{g}{\cos(\beta_\mu)}\sin(\beta + \beta_\mu)$$

[1]This chapter is based on a paper: McIntyre, M., Vahidi, A., and Dawson, D., "An Online Estimator for Heavy Vehicles Mass and Road Grade" *Proceedings of IMEC*, Chicago, Il, 2006. The original publication is copyrighted by ASME.

The following assumptions are made to facilitate the design of the estimator.

Assumption 1: The road grade $\beta(t)$ varies continuously with vehicle longitudinal position if the velocity of vehicle $v(t)$ is a continuous function of time, i.e. $\dot{\beta}(t) \in \mathcal{L}_\infty$.

Assumption 2: The signals $v(t)$, $\dot{\omega}_e(t)$, $T_e(t)$ and gear number are measurable.

Assumption 3: The values of the the engine crankshaft inertia J_e, the coefficient of rolling resistance μ and drag coefficient C_d, are known and remain constant with time.

Assumption 4: For second stage, the mass of the vehicle is a known constant and the road grade $\beta(t)$ varies with time very slowly, i.e. rate of change of $\beta(t)$ is almost equal to zero $\left(\dot{\beta}(t) \approx 0\right)$.

Assumption 5: It is assumed that the clutch is always fully engaged and friction brakes are never applied. These assumptions are not valid during the gearshift and braking periods. Unfortunately in a standard setting the service brake pressure and subsequently the brake torques cannot be accurately determined. Developing an accurate model of the transmission and the gear shift process is an option but overcomplicates the model used for estimation. To address this issues later pre- and post-conditioning of the signals and the estimates are proposed to handle periods of gearshift and braking.

In equation (2.2) $\tan(\beta_\mu) = \mu$. We can rewrite equation (2.2) in the following form,

$$y = \phi^T \theta,\ \phi = [\phi_1, \phi_2]^T\ \theta = [\theta_1, \theta_2]^T \tag{4.1}$$

where

$$\theta = [\theta_1, \theta_2]^T = [\frac{1}{M},\ \sin(\beta + \beta_\mu)]^T \tag{4.2}$$

are the unknown parameters of the model and this algorithm is developed to estimate those parameters and

$$y = \dot{v},\ \phi_1 = \frac{T_e - J_e\dot{\omega}}{r_g} - F_{fb} - F_{aero},\ \phi_2 = -\frac{g}{\cos(\beta_\mu)} \tag{4.3}$$

can be calculated based on measured signals and known variables.

4.2 Adaptive Least-Squares Estimator For Estimating Vehicle Mass

A *prediction error* $\varepsilon(t) \in \mathbb{R}$ is defined as the difference between measured acceleration and estimated acceleration using equation (2.2),

$$\varepsilon \triangleq y_f - \hat{y}_f \tag{4.4}$$

Here the subscript f denotes a filtered signal. The measured acceleration y is filtered by a first-order low-pass filter,

$$\dot{y}_f = -\alpha_o y_f + \alpha_o y \tag{4.5}$$

where $y_f(t_0) = 0$, and α_0 is the filter's constant.

The filtered estimated longitudinal acceleration $\hat{y}_f(t)$, in equation (4.4) is related to the parameter estimates $\hat{\theta} = \begin{bmatrix} \hat{\theta}_1 & \hat{\theta}_2 \end{bmatrix}^T$ as follows,

$$\hat{y}_f = \phi_f \hat{\theta} \tag{4.6}$$

where $\phi_f(t) \in \mathbb{R}^{1\times 2}$ is the regression vector filtered by the same low-pass filter described in (4.5) and the initial condition for ϕ_f, $\phi_f(t_0) = \begin{bmatrix} 0 & 0 \end{bmatrix}$.
Using the above equations, the prediction error dynamics are described by,

$$\dot{\varepsilon} + \alpha_0 \varepsilon = \frac{d}{dt}\left(\phi_f \tilde{\theta}\right) + \alpha_0 \phi_f \tilde{\theta} \tag{4.7}$$

where $\tilde{\theta}(t)$ is the error in parameter estimates defined as,

$$\tilde{\theta} \triangleq \theta - \hat{\theta}. \tag{4.8}$$

Therefore from (4.7), the prediction error $\varepsilon(t)$ is related to parameter estimation error,

$$\varepsilon = \phi_f \tilde{\theta}. \tag{4.9}$$

This equation is used for the first stage of estimation for which a continuous version of recursive least square is used. The parameter update law is [24],

$$\dot{\hat{\theta}} \triangleq -K_{ls} \frac{P_{ls}\phi_f^T \varepsilon}{1+\gamma\phi_f P_{ls}\phi_f^T} \tag{4.10}$$

where $K_{ls} \in \mathbb{R}^{2\times 2}$ is a constant diagonal gain matrix, γ is a constant tunable gain, $\varepsilon(t)$ is defined in equation (4.4), ϕ_f is the regression vector, and $P_{ls}(t) \in \mathbb{R}^{2\times 2}$ is the covariance matrix. The covariance matrix $P_{ls}(t)$ is updated at every step and recursively as follows,

$$\dot{P}_{ls} \triangleq -K_{ls} \frac{P_{ls}\phi_f^T \phi_f P_{ls}}{1+\gamma\phi_f \phi_f^T} \tag{4.11}$$

where the initial condition of P_{ls} is given by, $P_{ls}(t_o) = k_0 I_{2\times 2} and\ k_0$ is a constant positive gain. The estimated vehicle mass $\hat{M}(t)$ is the inverse of $\hat{\theta}_1$,

$$\hat{M} = \frac{1}{\hat{\theta}_1} \tag{4.12}$$

and an initial estimate of road grade $\hat{\beta}(t)$ is given by,

$$\hat{\beta} \triangleq \sin^{-1}\left(\hat{\theta}_2\right) - \beta_\mu. \tag{4.13}$$

The first stage estimator assumes a constant road grade. A second-stage nonlinear estimator is developed next to calculate a more accurate estimate when the grade is time-varying.

4.3 A Nonlinear Estimator for Estimating Road Grade

A Lyapunov-based estimator design is presented that receives the vehicle CAN signals and the mass estimate from the first stage and generates an estimate for the road-grade.
The longitudinal dynamics of the vehicle from equation (2.2) is rewritten as,

$$y = \phi_1 \theta_1 + f \tag{4.14}$$

where $\phi_1(t)$ and θ_1 were defined in equations (4.3) and (4.2) respectively. The term $f(t)$ represents the remaining $(\phi_2\theta_2)$ from the longitudinal dynamic model as defined in equation (2.2),

$$f \triangleq \frac{-g}{\cos(\beta_\mu)} \sin(\beta + \beta_\mu). \tag{4.15}$$

In the first stage, the prediction error $\varepsilon(t)$ was defined as the difference between estimated acceleration and actual acceleration. Here we define the velocity estimation error $e(t)$ as,

$$e \triangleq v - \hat{v} \tag{4.16}$$

where $\hat{v}(t)$ is the estimated velocity and is estimated using the following equation,

$$\hat{v} = \int_{t_0}^{t_f} \phi_1(t)\,\theta_1(t)\,dt + \int_{t_0}^{t_f} \hat{f}(t)\,dt \tag{4.17}$$

where $\hat{f}(t)$ is an estimate for $f(t)$; its calculation is explained next.
Differentiation with respect to time of (4.16) yields,

$$\dot{e} = \dot{v} - \dot{\hat{v}}. \tag{4.18}$$

From equation (4.17) we have,

$$\dot{\hat{v}} = \phi_1 \theta_1 + \hat{f}. \tag{4.19}$$

Substituting values of $\dot{v}$ and $\dot{\hat{v}}$ from equations (4.14) and (4.19) into (4.18), results in the following simplified form,

$$\dot{e} = \tilde{f} \tag{4.20}$$

where $\tilde{f}(t)$ is the estimator error defined as,

$$\tilde{f} \triangleq f - \hat{f}. \tag{4.21}$$

Finally we propose a proportional-integral nonlinear estimator for estimating $f(t)$,

$$\hat{f} = (k_1 + 1)\left[e(t) - e(T_{ls}) + \int_{t_0}^{t} e(\sigma)\, d\sigma\right] + \int_{t_0}^{t} k_2 \mathrm{sgn}(e(\sigma))\, d\sigma \tag{4.22}$$

where k_1, $k_2 \in \mathbb{R}^+$ are constant gains, and $sgn(.)$ denotes the signum function. Once $f(t)$ is estimated above, an estimate for the time-varying road grade can be obtained from equation (4.15) and is,

$$\hat{\beta} = \sin^{-1}\left(-\frac{\hat{f}}{g}\cos(\beta_\mu)\right) - \beta_\mu. \tag{4.23}$$

The convergence can be proven provided that value of k_2 is selected such that the following sufficient condition is satisfied,

$$k_2 > \left|\dot{f}(t)\right| + \left|\ddot{f}(t)\right|. \tag{4.24}$$

Based on Assumption 1 it can be shown that there exist an upper bound for $\dot{f}(t)$ and $\ddot{f}(t)$ and therefore a finite value for k_2 that meets this condition always exists. The proof is shown next.

4.4 Proof of Convergence

Lets define an auxiliary error term $s(t)$ as,

$$s \triangleq \dot{e} + e. \tag{4.25}$$

Taking the time derivative of (4.25) and substituting the values of $\ddot{e}$ we can write the dynamic expression for $s(t)$ as,

$$\dot{s} = \dot{f} - (k_1 + 1)\, s - k_2 \mathrm{sgn}(e) + \dot{e} \tag{4.26}$$

We would like to show that the estimate $\hat{f}(t)$ from the nonlinear estimator defined in equation (4.22) converges to actual value $f(t)$:

$$\hat{f}(t) \to f(t) \text{ as } t \to \infty \tag{4.27}$$

For the convergence proof a nonnegative Lyapunov function $V(t)$ is selected as,

$$V = \frac{1}{2} e^2 + \frac{1}{2} s^2 \tag{4.28}$$

where $e(t)$ and $s(t)$ are defined in equations (4.16) and (4.25) respectively. Taking the derivative of equation (4.28) with respect to time and using equations (4.25) and (4.26), we obtain,

$$\begin{aligned} \dot{V}(t) = \quad & e\,(s - e) \\ & + s\left(\dot{f} - (k_1 + 1)s - k_2 \mathrm{sgn}(e) + \dot{e}\right). \end{aligned} \tag{4.29}$$

Using the auxiliary error defined in equation (4.25), a simplified form of equation (4.29) can be written as,

$$\begin{aligned} \dot{V}(t) = \quad & -e^2 - k_1 s^2 + \dot{e}\dot{f} + e\dot{f} \\ & - k_2\,(\dot{e} + e)\,\mathrm{sgn}(e). \end{aligned} \tag{4.30}$$

Taking integral of equation (4.30) from t_0 to t yields,

$$\begin{aligned} V(t) \quad \leq \quad & V(t_0) - \int_{t_0}^{t} |e(\sigma)|^2 \, d\sigma \\ & - k_1 \int_{t_0}^{t} |s(\sigma)|^2 \, d\sigma + \int_{t_0}^{t} \dot{e}(\sigma)\dot{f}(\sigma) d\sigma \\ & - k_2 \int_{t_0}^{t} \dot{e}(\sigma)\mathrm{sgn}(e(\sigma)) d\sigma \\ & + \int_{t_0}^{t} e(\sigma)\left(\dot{f}(\sigma) - k_2 \mathrm{sgn}(e(\sigma))\right) d\sigma. \end{aligned} \tag{4.31}$$

After integrating the fourth term of the above by parts and the fifth term over time, we get,

$$\begin{aligned} V(t) \quad \leq \quad & V(t_0) - \int_{t_0}^{t} |e(\sigma)|^2 \, d\sigma + e(t)\dot{f}(t) \\ & -k_1 \int_{t_0}^{t} |s(\sigma)|^2 \, d\sigma - e(t_0)\dot{f}(t_0) \\ & +k_2 e(t_0)\text{sgn}(e(t_0)) - k_2 e(t)\text{sgn}(e(t)) \\ & + \int_{t_0}^{t} e(\sigma)\left(\dot{f}(\sigma) - \ddot{f}(\sigma) - k_2 \text{sgn}(e(\sigma))\right) d\sigma. \end{aligned}$$

If k_2 is selected such that,

$$k_2 > \left|\dot{f}(t)\right| + \left|\ddot{f}(t)\right|. \tag{4.32}$$

then the expression for $V(t)$ can be further simplified to,

$$V(t) \leq -k_0 \int_{t_0}^{t} |s(\sigma)|^2 \, d\sigma - \int_{t_0}^{t} |e(\sigma)|^2 \, d\sigma + C \tag{4.33}$$

where C is a boundary constant and can be defined as,

$$C \triangleq V(t_0) - e(t_0)\left(\dot{f}(t_0) - k_2 \text{sgn}(e(t_0))\right). \tag{4.34}$$

From the structure of (4.33) and the definition in (4.34), it is proven that $V(t) \in \mathcal{L}_\infty$; hence, $s(t)$, $e(t) \in \mathcal{L}_\infty$. Since $s(t)$, $e(t) \in \mathcal{L}_\infty$, (4.25) can be used to prove that $\dot{e}(t) \in \mathcal{L}_\infty$. From Assumption 1, and the definition in (4.15), it is possible to demonstrate that $\dot{f}(t) \in \mathcal{L}_\infty$. From the fact that $\dot{f}(t)$, $s(t)$, $e(t)$, and $\dot{e}(t) \in \mathcal{L}_\infty$, it is clear from (4.26) that $\dot{s}(t) \in \mathcal{L}_\infty$. The inequality defined by (4.33) can be used to prove that $s(t)$, $e(t) \in \mathcal{L}_2$. Since $s(t)$, $e(t)$, $\dot{s}(t)$ and $\dot{e}(t) \in \mathcal{L}_\infty$ and $s(t)$, $e(t) \in \mathcal{L}_2$, then Barbalat's Lemma can be used to prove that $|s(t)|$ and $|e(t)| \to 0$ as $t \to \infty$, and based on (4.20) and (4.21), it is clear that $\hat{f}(t) \to f(t)$ as $t \to \infty$.

Chapter 5

Refinement of Algorithm II and Results

To validate and fine-tune the second algorithm, we have used the three experimental data sets presented in section 3.1. First results with the original version of algorithm II are presented and the problems are discussed. Next refinements are proposed which improve the outcome of estimation.

5.1 Initial Results and the Issues of Algorithm II

First Algorithm II is implemented in its originally developed form with minor changes. In this case whenever brakes are applied, we have assumed zero brake pressure values whereas we had assumed constant brake pressure values in the first algorithm. Also algorithm II is not initialized by a batch; it runs recursively from start. Figure 5.1 shows the grade and mass estimation results for the data set-1. It can be seen that, although not very fast but very consistently the mass estimate is converging to the actual value with time, and hence the grade estimates is getting closer to the actual value of grade. The percent mass error at the end of the cycle is around 30%. The grade estimates seem to be smoother than those obtained by algorithm I; however spikes can be seen which may be again attributed to the gear shift. At this stage the estimator is not turned off when the clutch is

disengaged. The gain values used for data set-1 are $K_{ls} = \begin{pmatrix} 40 & 0 \\ 0 & 25 \end{pmatrix}$, $k_1 = 5$, $k_2 = 10$ and $\beta = 10$.

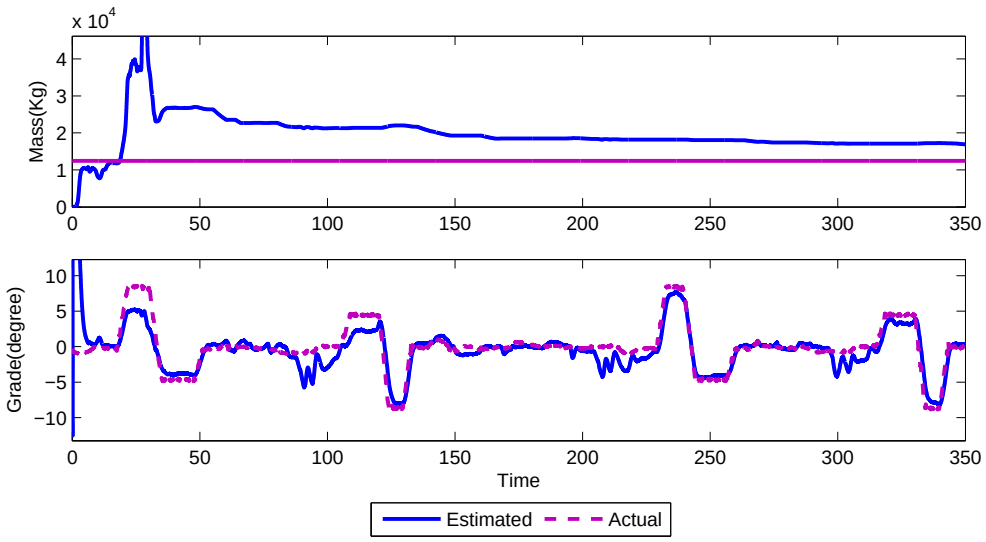

Figure 5.1: Estimated road grade and mass with algorithm II for data set-1.

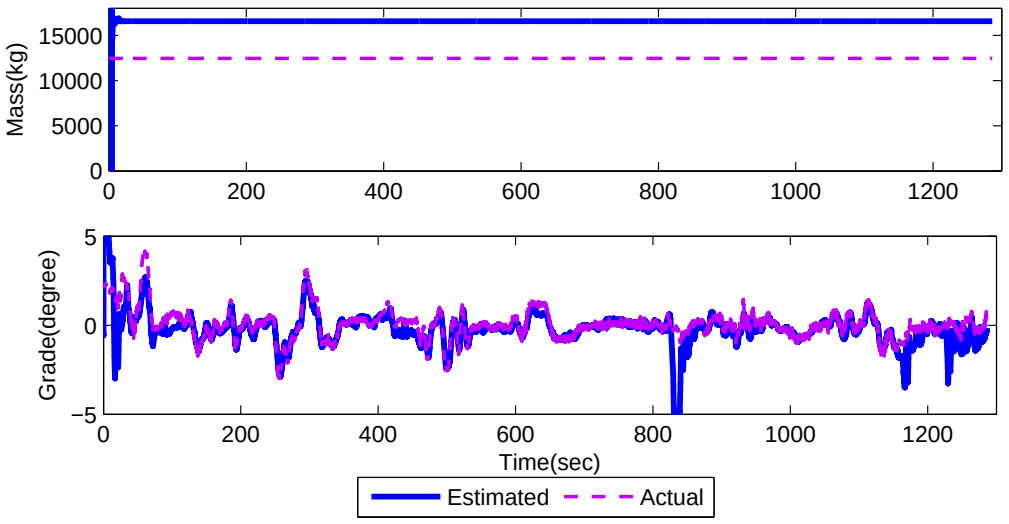

Figure 5.2: Estimated road grade and mass with algorithm II for data set-2.

Figures 5.2 and 5.3 show initial results for data sets 2 and 3 respectively using second algorithm. For data set-2 percent error in mass is around 30%. Even though the percent error in

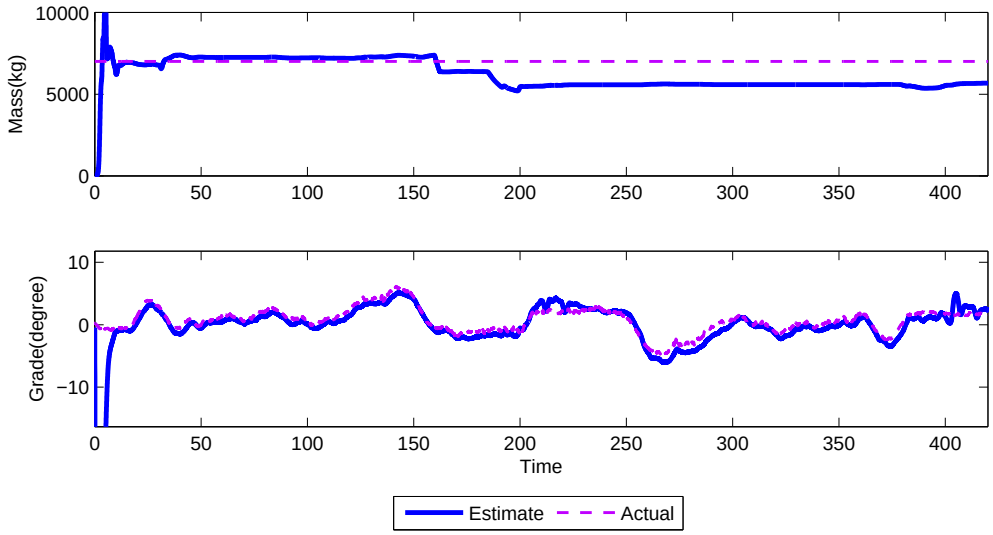

Figure 5.3: Estimated road grade and mass with algorithm II for data set-3.

mass is around 30%, the grade estimate follows the actual grade closely. For data set-3 the percent error in estimated mass is around 20% at the end of first cycle but grade estimate follows the actual grade profile closely. For data sets-2 and 3 the estimator gains are the same as data set-1, however the filter constant had to be changed to $\beta = 5$ for the reported results.

The main issue detected during simulation seems to be robustness of algorithm 2 to selection of estimator gains. Also unknown brake pressure values and model mismatch during gear shift result in deviation of estimation from actual value when brake is applied or clutch is not fully engaged (in particular notice the spikes in estimate of road grade in figures 5.2 and 5.1). The small signal-to-noise ratio for some of the signals is also a major challenge. Another issue with the original code of algorithm II is the computational time which is well-above the real-time requirements. For a 400-second window of real-time data set, the original estimation time took more than 90 minutes. In order for the algorithm to be real-time implementable it is necessary to optimize the estimation code.

5.2 Refinements to Algorithm II

As explained in the previous chapter, there are two stages to algorithm II: The first stage estimates mass of the vehicle recursively. Based on the mass estimate the second stage estimates the road grade using the nonlinear estimator (4.3). Preliminary results show that once a fairly good mass estimate is obtained from stage 1, the second stage estimates the grade fairly accurately and robustly. Considering this, most of our effort was focused toward improving the estimate of vehicle mass from first stage. This section explains the different directions explored.

Signal Filtering: Section 3.3 described the importance of filtering when using experimental data. For example Figure (5.4) shows the unfiltered acceleration signal which is very noisy making acceleration-based estimation a real challenge. To reduce the noise level in the measured signals we have used a low-pass filters to filter engine torque, velocity, and acceleration before feeding them to the estimator. Also the generated grade estimate is passed through another low-pass filter. For engine torque and velocity a second-order low-pass butterworth filter with cut-off frequency of $3rad/sec.$ is used. The acceleration signal is filtered using a first-order low-pass filter as shown in equation (4.5).

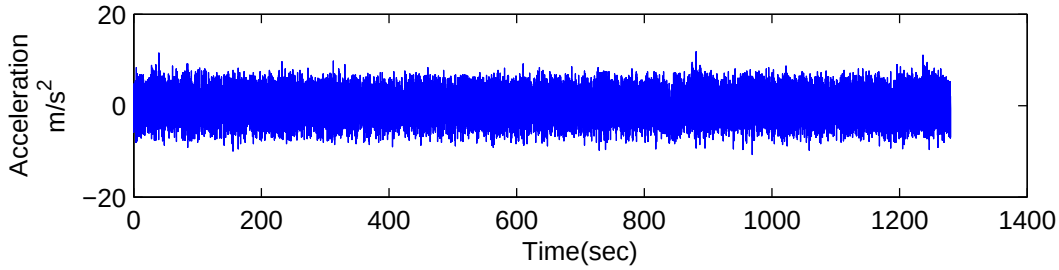

Figure 5.4: Unfiltered acceleration for data set-2.

Estimation Hold During Braking and Gearshift: The brake pressure values and therefore brake torques are not standard measurements and not available to us. Unknown brake torque can "confuse" the estimator when brakes are applied. To circumvent this problem, while the estimation process continues with the assumption of zero-brake torque, the estimation results are discarded and the mass and grade estimates are not updated. Updating of mass and grade estimates is resumed

when the brakes are released. Also during gearshift period, the clutch is completely or partially disengaged disrupting the flow of power to the wheels. Therefore during this period the simple longitudinal dynamics we have used does not predict the torque at the wheel accurately. Again the mass and grade estimates are not updated during clutch disengagement. Updating is resumed a few seconds after clutch is re-engaged to ensure that the induced vibrations in the driveline are damped.

Covariance Resetting: The recursive least square's covariance matrix dies with time and makes it impossible to track changes in mass that occur after each loading and unloading of the truck. To remedy this we reset the covariance matrix in the beginning of each trip while using the previous estimates as the initial values for the estimator.

Reduced Computation Time: As explained in section previous section, computational time of the algorithm was very large. By optimizing the estimator code, relying more on SIMULINK blocks and minimizing use of MATLAB function blocks we have been able to reduce the execution time of the algorithm by more than 10 folds. As a result the algorithm can now run in real-time. The pre and post-processing of signals is now streamlined such that the code is ready for on-vehicle testing which is being considered as a next step.

5.3 Results with the Refined Algorithm

5.3.1 Simulation Results

The refined estimator is first tested using simulated data. Two simulated data sets are created, one with step changes in road grade and one with sinusoidal grade variation. A constant vehicle mass of M=20,000 kg is assumed for both data sets. Persistent excitation is required for accurate estimation of parameters and this is enforced by choice of a sufficiently varying fueling profile. The engine torque signal is calculated based on this fueling command; in addition a random noise signal was added to the torque signal to reflect a more realistic situation. It was assumed that brakes are not applied and there is no gearshift during simulation.

Figure 5.5 shows the estimation results for step changes in road grade. The mass estimate

reaches within 10% of its actual value within 7 seconds. As mass estimate nears its actual value, the estimate of grade also tracks the actual grade closely. Figure 5.5 shows the same for sinusoidal variation of grade profile. Again after around 7 seconds, the mass estimate reaches within 10% of its value.

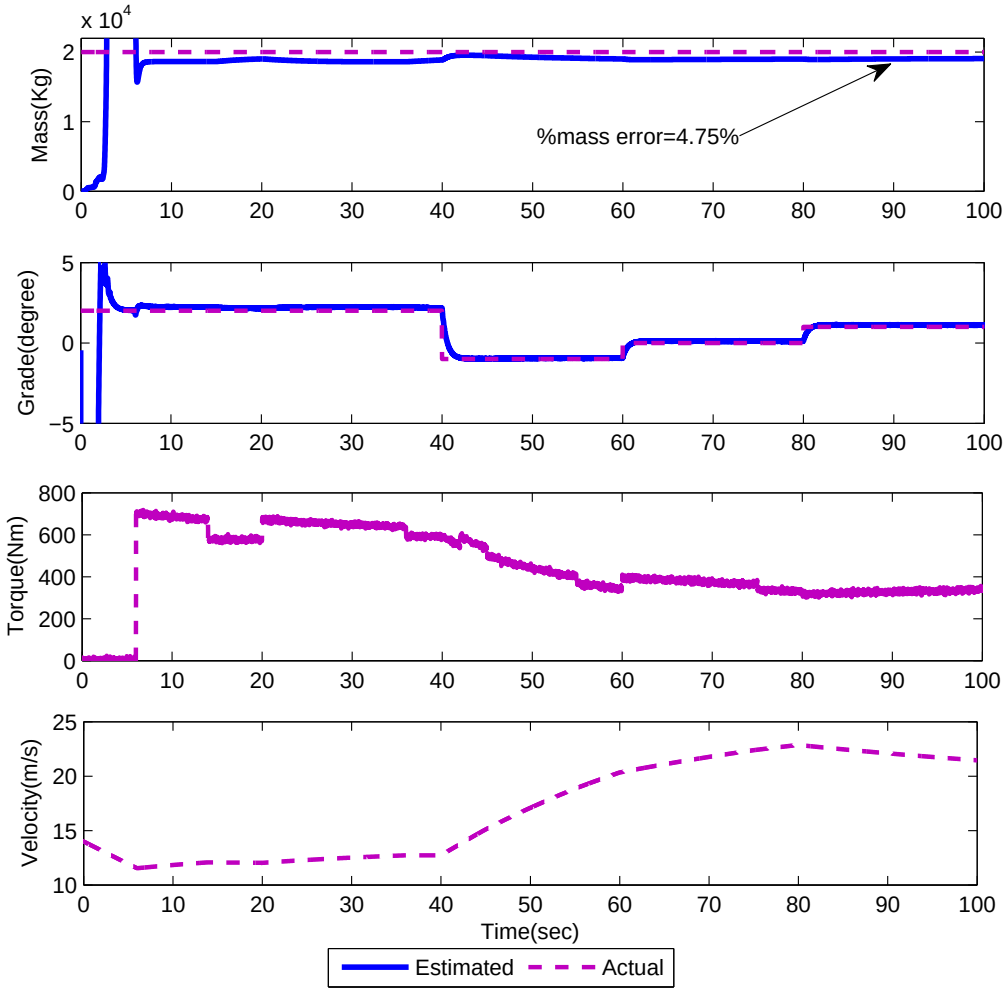

Figure 5.5: Estimate of mass and road grade compared to actual values for simulated data when grade is varied in steps.

5.3.2 Experimental Results

With the two-stage estimation strategy proven effective with simulated data, the algorithm

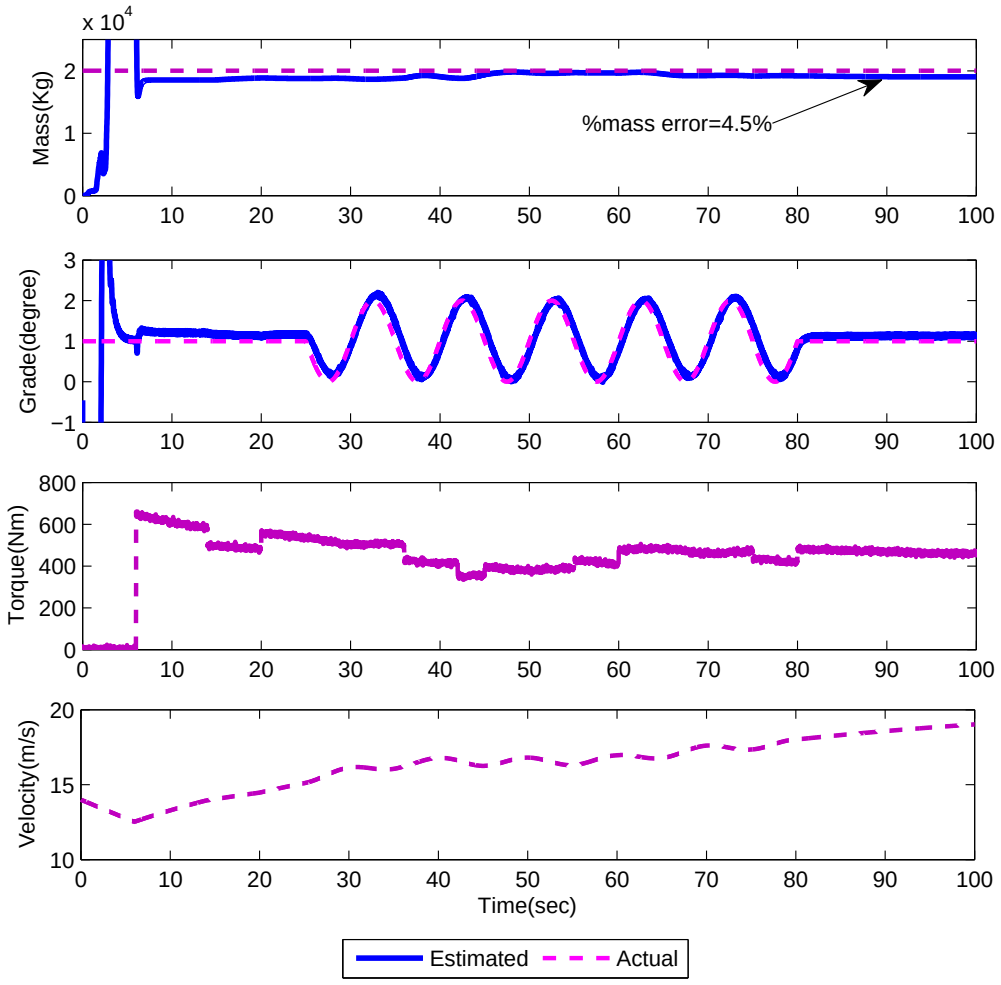

Figure 5.6: Estimate of mass and grade compared to actual values for simulated data when grade is varied sinusoidally.

was next tested with several experimental data sets. The experimental data sets were obtained at Eaton from a heavy duty vehicle with automated manual transmission. The data was obtained from Engine Control Module through J1939, and from driveline control module and from the clutch control module. The truck was driven on three different roads, Referred to as the data set 1 2 and 3. Each experimental run was selected to demonstrate varying road and load conditions. At each experimental run, the total vehicle mass was modified by changing the payload, and was known *a priori*.

For all experimental runs, the least-squares estimator gains were chosen to be

$$\begin{aligned} \beta_0 &= 5, \gamma = 5 \\ K_{ls} &= diag\{69, 40\} \\ P_{ls}(t_0) &= diag\{1, 1\} \end{aligned} \tag{5.1}$$

where $diag\{\cdot\}$ represents the diagonal elements of a 2×2 matrix. The nonlinear estimator had the following gain values

$$k_1 = 7 \text{ and } k_2 = 10.$$

5.3.2.1 Experiment 1: Data set-1

The total vehicle mass for this run was $M = 12,400[kg]$. Figure 5.7 illustrates the results of the least-squares mass estimator and the nonlinear road grade estimator. From Figure 5.7, it is clear that this strategy provides an accurate mass estimate $\hat{M}(t)$ owhen $t \geq 10[\text{sec}]$. Percent mass error for $t \geq 10[\text{sec}]$ is less then 4%. Compared to results from 5.1 estimate of mass converges to actual mass quickly and grade estimate also tracks the actual grade with good accuracy.

5.3.2.2 Experiment 2: Data set-2

The total vehicle mass was approximately $M = 12,400[kg]$. Figure 5.8 illustrates the results. Maximum percent error in mass after $20[\text{sec}]$ is less then 5%. Once the estimate of mass converges to actual mass, the nonlinear road grade estimator also tracks the actual grade closely. Implementing the refinements discussed in previous section, the spikes in road grade during braking and gear shifting periods are considerably reduced. This can be observed by a comparison to earlier results shown in Figure 5.2.

5.3.2.3 Experiment 3: Data set-3

For this run the truck was empty with the total mass $M = 7,000[kg]$. Figure 5.9 illustrates

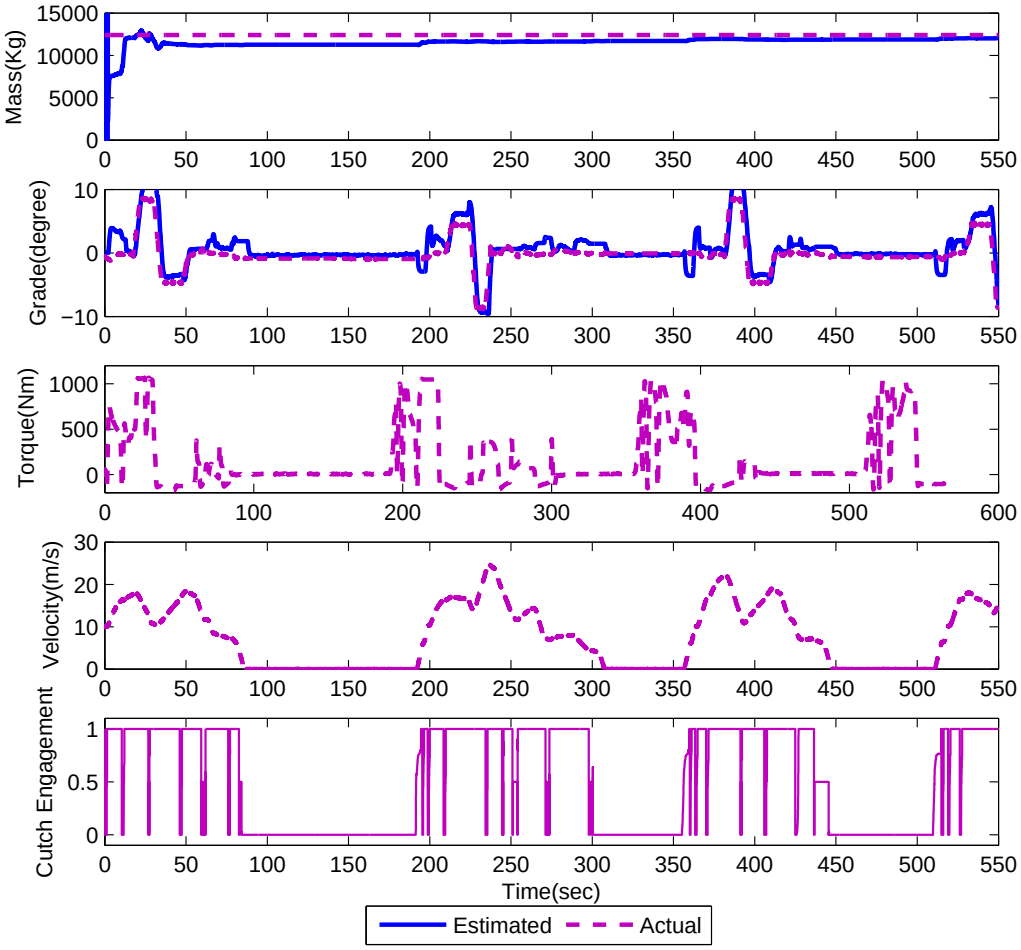

Figure 5.7: Estimation results for data set-1.

the results of the least-squares mass estimator and the nonlinear road grade estimator. Figure 5.9, again demonstrates good mass estimate; the maximum percent error in mass reduces to less then 4% in less than 10 seconds.

5.3.2.4 Experiment 4: sensitivity of the grade estimate to mass error

For this experiment, we investigate a potential weakness in our estimation scheme. Due to the fact that our two stage approach requires an estimation of the mass to subsequently estimate the road grade, we wanted to establish how sensitive the road grade estimation was to potential masses

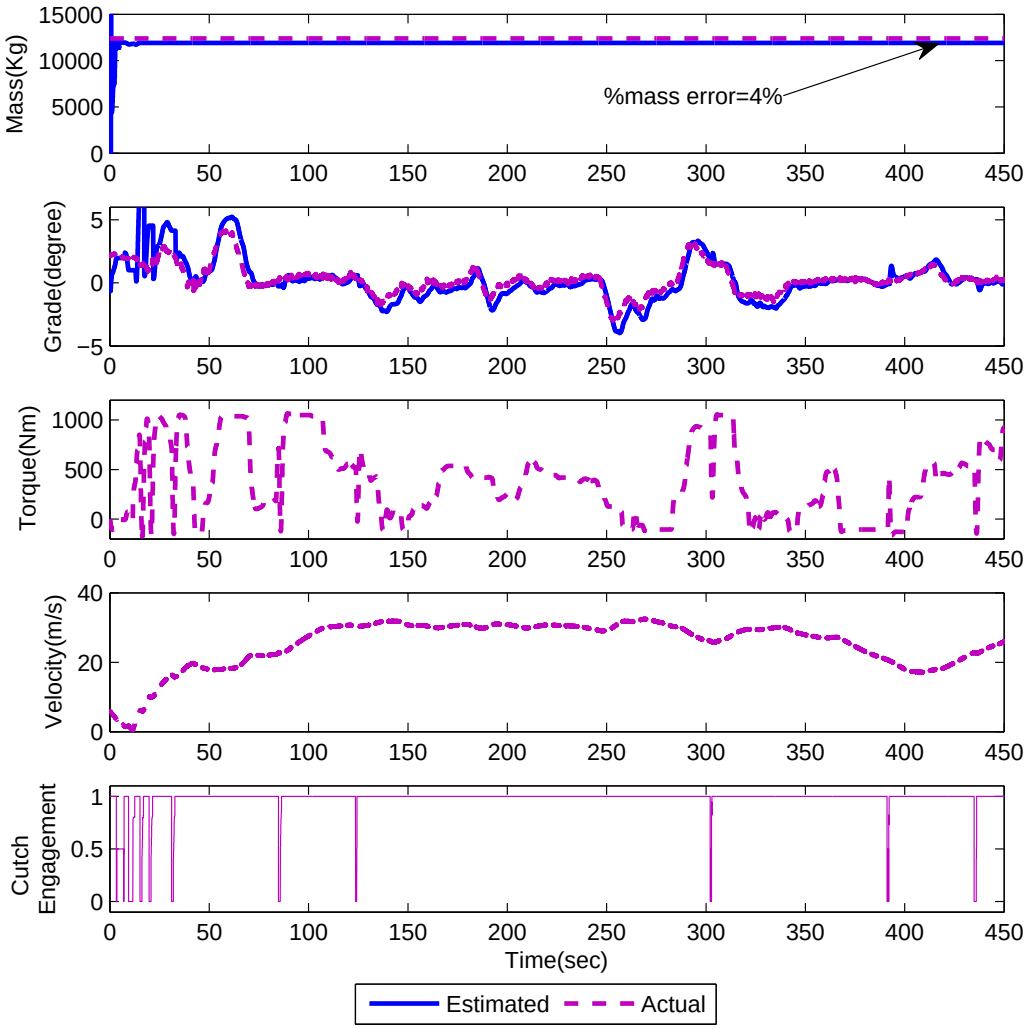

Figure 5.8: Estimation results for data set-2.

estimation error. With this in mind, we injected a mass estimation error and re-ran the data-set from Experiment 2. We introduced 15 and 20 percent mass estimation errors into the grade estimator. Figure 5.10 illustrates the effect the individual mass estimation error signals has on the road grade estimation $\hat{\beta}(t)$ when applied to the data set-2. From figure 5.10, it is clear that the injected mass estimation error does not influence $\hat{\beta}(t)$ significantly. Table 5.1 shows RMS error in estimated grade for different mass error. We have neglected the initial 50[sec] of data while calculating RMS error.

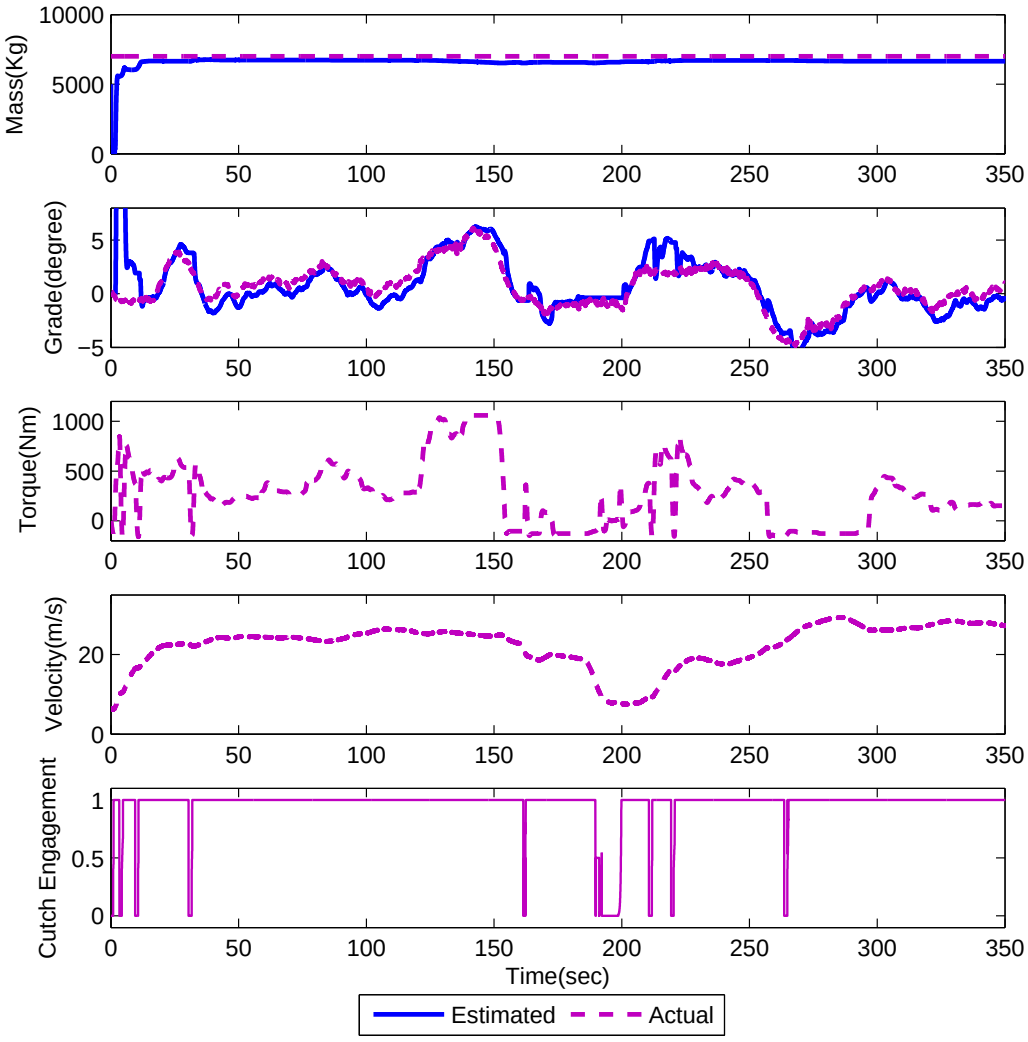

Figure 5.9: Estimation results for data set-3.

Table 5.1: RMS error in grade for different percent mass errors for data set-2

% Mass error	RMS error in grade
0%	0.55
15%	0.49
20%	0.49

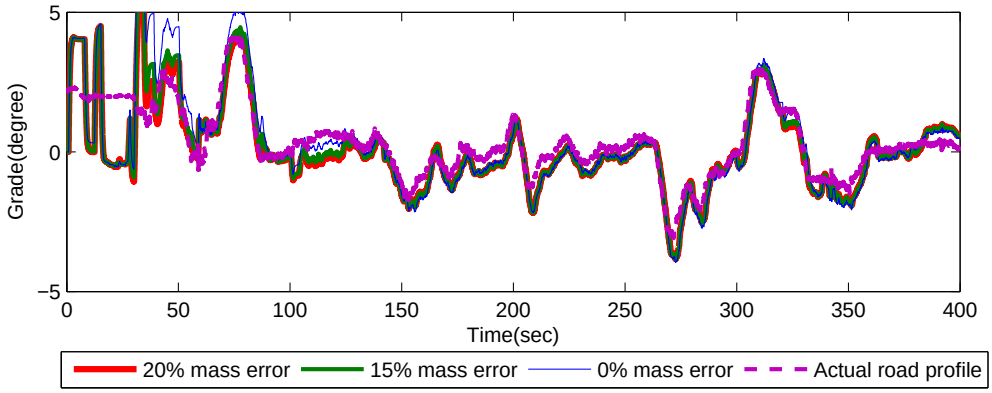

Figure 5.10: Sensitivity of the grade estimator to errors in mass estimate for data set-2.

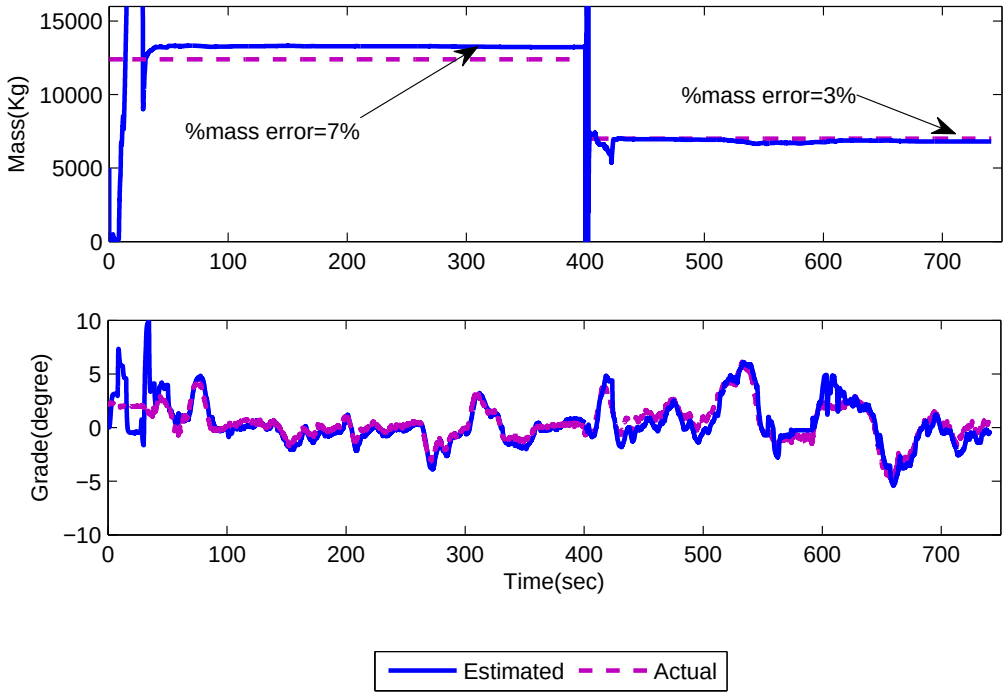

Figure 5.11: Estimation results when data sets 2 and 3 ran in series.

5.3.2.5 Experiment 5: Covariance resetting

To check robustness of the two-stage algorithm against changes in vehicle loading, data

set-2 was ran followed by data set-3. Mass of the truck for data set-2 is $M = 12,400[kg]$ and for data set-3 $M = 7,000[kg]$. Figure 5.11 shows result for estimated mass and grade as compared to the actual mass and grade profile. The spikes in estimate of mass when there is change in mass at around $t = 400[\text{sec}]$ is due to resetting the covariance matrix, which allows the estimate of mass to converge to the new mass value. Estimate of grade also follows the actual grade very closely.

5.4 Future Research For Algorithm II

Overall it seems that algorithm II is more robust than algorithm I as its convergence does not depend on initialization nor is as sensitive to the estimator parameters. The following issues should be addressed for further improvements:

Adaptive Parameter set for K_{ls}: We explored the possibility of adapting the gain K_{ls}; the values of empty truck mass and maximum possible mass are known and this information may be utilized when adapting K_{ls}. If the estimate of mass is grater then maximum possible value, K_{ls} is selected in such a way that it forces the estimate of mass to remain below upper bound of mass and when the estimate of mass goes below the mass of empty truck, K_{ls} is selected in such a way that it pushes the estimate of mass to go above the lower bound. We believe there is room for improvement by adaptation of K_{ls} or other gains.

Persistent excitation condition for initialization: The original algorithm was very sensitive to persistent excitation of incoming data. To remedy this we have added conditions that check the velocity and acceleration levels and when low the algorithm is turned of. The result has been promising however there is still room for including additional and more restrictive logic that check the quality of incoming signals and stop algorithm during poor excitation periods.

Real time implementation: We are able to demonstrate the performance of two-stage estimation strategy by getting accurate results for multiple simulated as well as experimental data sets. Now the next step is to test the algorithm in a real-time scenario. Testing of the algorithm in real-time scenario will be carried out at the Eaton Corporation (project partner) facility.

Chapter 6

Conclusion and Future Work

Estimation of the vehicle mass and time-varying road grade simultaneously is a challenging problem. Most of the existing work in the literature focuses on only estimating one of the parameters. In practice however estimation of one can not be completed without the knowledge of the other. The novelty of the algorithms outlined in this thesis is simultaneous estimation of both unknowns. First we have validated the powertrain model by comparing the model velocity with the measured velocity. We then presented the estimation results using two algorithms and presented new fixes and refinements to improve the estimation quality. A major hurdle with the first algorithm was the spikes in the grade estimate which was overcome by turning off the estimator during clutch disengagement. Proper initialization of the recursive estimator by intelligent selection of the batch size remains a good direction for future research. During the course of tests with algorithm I we have also studied several other issues for example the appropriate filters and their bandwidth for reducing the influence of signal noise and also use of a torque sensor to validate the engine torque readings.

The second two-stage algorithm proved very promising. We have been able to show its relatively robust performance using a number of experimental data sets. The major issue in the second algorithm was the spikes in the grade estimates during braking and gearshift. This issue was resolved by holding the estimate update during periods of braking and clutch disengagement.

We have also faced and resolved several other issues for example selecting the appropriate filters that reduce the influence of signal noise on the final estimation results and improving the speed of estimator convergence and its computation time.

The algorithms are now more robust and can be tested in real-time in the next step. We believe there is still room for improvement in both the algorithms in the following areas:

First algorithm: Selecting an adaptive batch size based on persistent excitation condition of incoming data and time-varying forgetting factors are important areas for further investigation. Fixed batch size can be replaced by adaptive batch size to ensure the convergence of estimation results to actual values for all the experimental data sets with the same setup. Covariance resetting is one of the areas of interest for further investigation. This will ensure that the algorithm doesn't lose its sensitivity to new incoming data and can track changes in parameters. Spikes during gear shifting and braking periods are reduced significantly but still there are frequent spikes in estimate of road grade, may be reduced by augmenting a model of transmission with the longitudinal dynamics model.

Second algorithm: Compared to first algorithm, this algorithm is much more robust and produces accurate results for multiple data sets with the same setup of initial conditions and gains. This algorithm is ready for testing in real-time scenario but adaptation of the gain K_{ls} and adding more checks on persistent excitation condition can improve the estimation results and can increase the robustness of the algorithm. For example the gain K_{ls} can be adapted to ensure mass estimate remains between feasible upper and lower bounds.

We are now filtering the data in both algorithms using fixed-gain low-pass filters. Use of bandpass and low-pass filters with adaptive parameters is another direction to investigate. In adaptive filtering, transfer function of a filter is selected based on perceived noise level of incoming signal and best filter is selected accordingly.

Also the results presented in this thesis are produced without the knowledge of braking forces and accurate powertrain model. It would be interesting to see the results when accurate powertrain model along with all braking forces are available.

Bibliography

[1] A. Astrom and B. Wittenmark. *Adaptive Control*. Addison Wesley, second edition, 1994.

[2] M. S. de Queiroz B. Xian and D. M. Dawson. A continuous control mechanism for uncertain nonlinear systems. *Optimal Control Stabilization and Nonsmooth Analysis, Lecture Notes in Control and Information Sciences*, 4:251–262, 2004.

[3] H.S. Bae and J. Gerdes. Parameter estimation and command modification for longitudinal control of heavy vehicles. *Proceedings of International Symposium on Advanced Vehicle Control*, 2000.

[4] H.S. Bae, J. Ryu, and J. Gerdes. Road grade and vehicle parameter estimation for longitudinal control using GPS. *Proceedings of IEEE Conference on Intelligent Transportation Systems*, 2001.

[5] S. Bittani, P. Bolzern, and M. Campi. Convergence and exponential convergence of identification algorithms with directional forgetting factor. *Automatica*, 26, 5:929–932, 1990.

[6] S. Bittani, P. Bolzern, M. Campi, and E. Coletti. Deterministic convergence analysis of RLS estimators with different forgetting factors. *Proceedings of the 27th Conference on Decision and Control*, pages 1530–1531, 1988.

[7] Liyu Cao and Howard M. Schwartz. A novel recursive algorithm for directional forgetting. *Proceedings of the American Control Conference*, pages 1334–1338, 1999.

[8] M. Druzhinina, L. Moklegaard, and A. Stefanopoulou. Compression braking control for heavy-duty vehicles. *Proceedings of American Control Conference*, 2000.

[9] M. Druzhinina, A. Stefanopoulou, and L. Moklegaard. Adaptive continuously variable compression braking control for heavy-duty vehicles. *ASME Dynamic Systems, Measurement and Control*, 124:406–414, 2002.

[10] T.R. Fortescue, L.S. Kershenbaum, and B.E. Ydstie. Implementation of self-tuning regulators with variable forgetting factors. *Automatica*, 17, 6:831–835, 1981.

[11] T. Hagglund. Recursive estimation of slowly time-varying parameters. *Proceedings of IFAC*, pages 1137–1142, 1985.

[12] P. Ioannou and Z. Xu. Throttle and brake control systems for automatic vehicle following. *PATH Research Report UCB-ITS-PRR-94-10*, 1994.

[13] C.R. Johnson. *Lectures on Adaptive Parameter Estimation*. Prentice Hall, 1988.

[14] R. Kulhavy. Restricted exponential forgetting in real-time identification. *Proceedings of IFAC*, pages 1143–1148, 1985.

[15] M.K. Liubakka, D.S. Rhode, J.R. Winkelman, and P.V. Kokotovic. Adaptive automotive speed control. *IEEE Transactions on Automatic Control*, 38, 7:146–156, 1993.

[16] M. McIntyre, A. Vahidi, and D. Dawson. An online estimator for heavy vehicle's mass and road grade. *Proceedings of ASME International Mechanical Engineering Congress and Exposition*, 2006.

[17] K. Oda, H. Takeuchi, M. Tsujii, and M. Ohba. Practical estimator for self-tuning automotive cruise control. *Proceedings of the American Control Conference*, pages 2066–2071, 1991.

[18] H. Ohnishi, J. Ishii, M. Kayano, and H. Katayama. A study on road slope estimation for automatic transmission control. *JSAE Review*, 21:322–327, 2000.

[19] J.E. Parkum, N.K. Poulsen, and J. Holst. Selective forgetting in adaptive procedures. *Proceedings of the 11th Triennial World Congress of the IFAC*, 2:137–142, 1990.

[20] Z. Qu and J. X. Xu. Model-based learning controls and their comparisons using lyapunov direct method. *Asian Journal of Control*, 4(1):99–110, 2002.

[21] Steiner Saelid, Olav Egeland, and Bjarne Foss. A solution to the blow-up problem in adaptive controllers. *Modeling, Identification and Control*, 6, 1:36–39, 1985.

[22] Steiner Saelid and Bjarne Foss. Adaptive controllers with a vector variable forgetting factor. *Proceedings of the 22nd IEEE Conference on Decision and Control*, pages 1488–1494, 1983.

[23] Mario E. Salgado, Graham C. Goodwin, and Richard H. Middleton. Modified least squares algorithm incorporating exponential resetting and forgetting. *International Journal of Control*, 47, 2:477–491, 1988.

[24] S. Sastry and M. Bodson. Adaptive control: Stability, convergence and robustness. 1989.

[25] N. Rao Sripada and D. Grant Fisher. Improved least square identification. *International Journal of Control*, 46, 6:1889–1913, 1987.

[26] A. Vahidi, M. Druzhinina, A. Stefanopoulou, and H. Peng. Simultaneous mass and time-varying grade estimation for heavy-duty vehicles. *Proceedings of American Control Conference*, 2003.

[27] A. Vahidi and W. Greenwell. A decentralized model predictive control approach to power management of a fuel cell-ultracapacitor hybrid. *Proceedings of the American Control Conference*, pages 5431–5437, 2007.

[28] A. Vahidi, A. Stefanopoulou, and H. Peng. Experiments for online estimation of heavy vehicle's mass and time-varying road grade. *Proceedings of IMECE*, 2003.

[29] A. Vahidi, A. Stefanopoulou, and H. Peng. Adaptive model predictive control for vehicle braking assist system design. *Proceedings of ASME International Mechanical Engineering Congress and Exposition*, 2004.

[30] A. Vahidi, A. Stefanopoulou, and H. Peng. Recursive least squares with forgetting for online estimation of vehicle mass and road grade: Theory and experiments. *Journal of Vehicle System Dynamics*, 43:31–57, 2005.

[31] V. Winstead and I.V. Kolmanovsky. Estimation of road grade and vehicle mass via model predictive control. *Proceedings of IEEE Conference on Control Applications*, 2005.

[32] M. Wuertenberger, S. Germann, and R. Isermann. Modelling and parameter estimation of nonlinear vehicle dynamics. *Proceedings of ASME Dynamical Systems and Control Division*, 44, 1992.

[33] D. Yanakiev, J. Eyre, and I. Kanellakopoulos. Longitudinal control of HDV's: Experimental evaluation. Technical Report MOU 293, PATH, 1998.

[34] Naoharu Yoshitani and Akihiko Hasegawa. Model-based control of strip temperature for the heating furnace in continuous annealing. *IEEE Transactions on Control Systems Technology*, 6, 2:146–156, 1998.